PREPARATION OF CHITOSAN-TITANIUM DIOXIDE BEADS FOR PHENOL DEGRADATION

Miss Punnida Nonsuwan

A Thesis Submitted in Partial Fulfillment of the Requirements
for the Degree of Master of Science Program in Biotechnology
Faculty of Science
Chulalongkorn University
Academic Year 2012

การเตรียมบีดไคโตซาน-ไททาเนียมไดออกไซด์สำหรับการสลายฟีนอล

นางสาวพรรณิดา นนสุวรรณ์

วิทยานิพนธ์นี้เป็นส่วนหนึ่งของการศึกษาตามหลักสูตรปริญญาวิทยาศาสตรมหาบัณฑิต
สาขาวิชาเทคโนโลยีชีวภาพ
คณะวิทยาศาสตร์ จุฬาลงกรณ์มหาวิทยาลัย
ปีการศึกษา 2555

Thesis Title	PREPARATION OF CHITOSAN-TITANIUM DIOXIDE BEADS FOR PHENOL DEGRADATION
By	Miss Punnida Nonsuwan
Field of Study	Biotechnology
Thesis Advisor	Assistant Professor Manchumas Prousoontorn, Ph.D.
Thesis Co-advisor	Krisana Siralertmukul, Ph.D.

Accepted by the Faculty of Science, Chulalongkorn University in Partial Fulfillment of the Requirements for the Master's Degree

…….Dean of the Faculty of Science

(Professor Supot Hannongbua, Dr. rer. nat.)

THESIS COMMITTEE

…….Chairman

(Professor Piamsook Pongsawasdi, Ph.D.)

…….Thesis Advisor

(Assistant Professor Manchumas Prousoontorn, Ph.D.)

…….Thesis Co-advisor

(Krisana Siralertmukul, Ph.D.)

…….Examiner

(Kittinan Komolpis, Ph.D.)

…….External Examiner

(Pornpimol Sritongkham, Ph.D.)

พรรณิดา นนสุวรรณ์ : การเตรียมบีดไคโตซาน-ไททาเนียมไดออกไซด์สำหรับการสลายฟีนอล. (PREPARATION OF CHITOSAN-TITANIUM DIOXIDE BEADS FOR PHENOL DEGRADATION) อ. ที่ปรึกษาวิทยานิพนธ์หลัก: ผศ. ดร.มัญชุมาส เพราะสุนทร, อ.ที่ปรึกษาวิทยานิพนธ์ร่วม: ดร.กฤษณา ศิรเลิศมุกุล, 104 หน้า.

ในงานวิจัยนี้ได้พัฒนาการสังเคราะห์บีดสามชนิดเพื่อใช้เป็นทางเลือกสำหรับการบำบัดฟีนอลในน้ำเสีย ทำการสังเคราะห์บีดไททาเนียมไดออกไซด์ผสมกับไคโตซาน และ บีดไททาเนียมไดออกไซด์ดัดแปรที่กราฟท์บนบีดไคโตซาน โดยไคโตซานทำหน้าที่เป็นตัวพยุงไททาเนียมไดออกไซด์ นอกจากนี้ทำการสังเคราะห์ไททาเนียมไดออกไซด์สเฟียร์โดยจะใช้ไคโตซานทำหน้าที่เป็นตัวยึดไททาเนียมไดออกไซด์ไว้ด้วยกัน จากนั้นทำการศึกษาการดูดซับและปฏิกิริยาสลายฟีนอลโดยแสงของไคโตซานและตัวเร่งปฏิกิริยาไททาเนียมไดออกไซด์ชนิดต่าง ๆ พบว่าบีดไททาเนียมไดออกไซด์ดัดแปรที่กราฟท์บนไคโตซานมีความสามารถในการกำจัดฟีนอลได้ดีที่สุด จึงเลือกมาทำการศึกษาถึงผลของความเข้มข้นของกลูทาราลดีไฮด์และเวลาที่ใช้ในการเชื่อมระหว่างกลูทาราลดีไฮด์และไททาเนียมไดออกไซด์ ในขั้นตอนของการดัดแปรไททาเนียมไดออกไซด์ พบว่าภาวะที่เหมาะสมในการดัดแปรไททาเนียมไดออกไซด์คือการใช้กลูทาราลดีไฮด์เข้มข้น 3.75% โดยบ่มเป็นเวลา 1 ชั่วโมง การสลายตัวของฟีนอลขึ้นอยู่กับหลายปัจจัย ได้แก่ ระยะห่างระหว่างหลอดยูวีและผิวหน้าของสารละลาย การกวนสารละลาย ความเข้มข้นของไททาเนียมไดออกไซด์ที่ใช้กราฟท์บนไคโตซานบีด อุณหภูมิในการทำปฏิกิริยา ความเข้มของแสงยูวี และความเข้มข้นเริ่มต้นของฟีนอล จากการทดลองพบว่าบีดไททาเนียมไดออกไซด์ดัดแปรที่กราฟท์บนไคโตซาน ที่ความเข้มข้นของไททาเนียมไดออกไซด์ดัดแปรเท่ากับ 1% (โดยน้ำหนักต่อปริมาตร) เป็นความเข้มข้นที่ดีที่สุดสำหรับการเกิดปฏิกิริยาเมื่อเทียบกับความเข้มข้นอื่น ๆ เมื่อเพิ่มระยะห่างระหว่างหลอดยูวีและผิวหน้าของสารละลาย และเพิ่มความเข้นข้นเริ่มต้นของฟีนอล มีผลทำให้การสลายตัวของฟีนอลลดลง ในขณะที่การเพิ่มอุณหภูมิของปฏิกิริยาและความเข้มของแสงทำให้ฟีนอลเกิดการสลายตัวมากขึ้น ทั้งนี้การกวนสารละลายในขณะเกิดปฏิกิริยาก็ช่วยเพิ่มการสลายตัวของฟีนอลเช่นกัน เมื่อทดสอบประสิทธิภาพของบีดไททาเนียมไดออกไซด์ดัดแปรที่กราฟท์บนไคโตซานดังกล่าวในการกำจัดฟีนอล พบว่ามีประสิทธิภาพลดลงเพียง 10% หลังผ่านการใช้ซ้ำ 5 ครั้ง

สาขาวิชา เทคโนโลยีชีวภาพ ลายมือชื่อนิสิต.....

ปีการศึกษา 2555 ลายมือชื่อ อ.ที่ปรึกษาวิทยานิพนธ์หลัก.....

ลายมือชื่อ อ. ที่ปรึกษาวิทยานิพนธ์ร่วม.....

5372507423: MAJOR BIOTECHNOLOGY
KEYWORDS: CHITOSAN / PHENOL / PHOTOCATALYTIC DEGRADATION / TITANIUM DIOXIDE

PUNNIDA NONSUWAN: PREPARATION OF CHITOSAN-TITANIUM DIOXIDE BEADS FOR PHENOL DEGRADATION. ADVISOR: ASST. PROF. MANCHUMAS PROUSOONTORN, Ph.D., CO-ADVISOR: KRISANA SIRALERTMUKUL, Ph.D., 104 pp.

In this research, three types of beads as alternative means for phenol treatment were developed. Titanium dioxide blended chitosan beads (chitosan-TiO_2) and modified titanium dioxide (TiO_2) grafted chitosan were synthesized through the use of chitosan as a recovery agent. In addition, TiO_2 spheres were prepared which exploited chitosan as a binder. The adsorption-photodegradation of phenol in the presence of chitosan and various UV irradiated titanium dioxide (TiO_2) catalysts was investigated. The results revealed that modified TiO_2 grafted chitosan beads showed the best ability to remove phenol. The effect of glutaraldehyde concentration and glutaraldehyde incubation time on the modification of TiO_2 was investigated. An optimum condition was to use 3.75% of glutaraldehyde and incubated for 1 h. The degradation of phenol depended on several parameters such as the distance between UV lamp and surface of the solution, agitation of solution, modified TiO_2 concentration that was grafted on chitosan beads, reaction temperature, light intensity and initial phenol concentration. The modified TiO_2 grafted on chitosan beads at 1% (w/v) of modified TiO_2 exhibited the best concentration for the degradation of phenol when compared with other concentrations. An increase of the distance between UV lamp and surface of the solution and initial phenol concentration showed a decrease of phenol photodegradation. On the other hand, when the reaction temperature and light intensity increased, the removal of phenol increased. Besides, the agitation of solution during the photodegradation process had an effect on the enhancement of phenol degradation. The efficiency of modified TiO_2 grafted chitosan beads at 1% (w/v) of modified TiO_2 to degrade phenol was about 10% decrease when they were reused after 5 times.

Field of Study: Biotechnology Student's Signature .....

Academic Year: 2012 Advisor's Signature .....

Co-advisor's Signature .....

ACKNOWLEDGEMENTS

This study could not be successful without the valuable advice of my advisor and my co-advisor. The author is highly thankful to Assistant Professor Dr. Manchumas Prousoontorn and Dr. Krisana Siralertmukul who advise on this research project for their assistance, guidance and good suggestion for solving a problem throughout this project. The author would like to thank Professor Dr. Piamsook Pongsawasdi, chairman of thesis committee, Dr. Kittinan Komolpis, thesis committee and Dr. Pornpimol Sritongkham, thesis external committee for their valuable advice comments, suggestions and assessing this research.

In addition, the author also acknowledges the Center of Chitin-Chitosan Biomaterial, Metallurgy and Materials Science Research Institute of Chulalongkorn University and Department of Biochemistry, Faculty of Science, Chulalongkorn University for providing the equipment, chemicals, and facilities. I thank the Development and Promotion of Science and Technology Talents Project or DPST scholarship for financial support. The author would like to give acknowledgement of Miss Kanitta Numun for helpful and technical advices.

Finally, I really grateful to my parents for their all along encourage, understanding and greatest support, and my friends for every spirit.

CONTENTS

CHAPTER **Page**

CHAPTER **Page**

LIST OF TABLES

LIST OF FIGURES

Figure **Page**

Figure **Page**

LIST OF ABBREVIATIONS

%	percentage
μm	micrometer (s)
A	absorbance
C_0	the initial phenol concentration
C_t	the concentration of phenol in solution at a given time
cm	centimeter
cm^{-1}	unit of wave number
^oC	degree Celsius (centrigrade)
D	the distance between UV lamp and the surface of the solution
%DD	degree of deacetylation
g	gram (s)
FTIR	Fourier Transform Infrared
h	hour (s)
kDa	kilodalton
kV	kilovolt
mL	milliliter (s)
ml/h	milliliter per hour
min	minute (s)
nm	nanometer (s)
pH	power of hydrogen ion or the negative logarithm (base ten)
SEM	Scanning Electron Microscopy
W	watt
w/v	weight/volume
w/w	weight/weight
XRD	X-ray diffraction

CHAPTER I

INTRODUCTION

Nowadays, water pollution is becoming a very serious problem that must be solved, especially wastewater from industries which are contaminated with fat, oil, insecticide, detergent, organic and inorganic substances. From the disclosure of Greenpeace Southeast Asia shows that each year the production and importation of chemical reagents for Thai industries are more than 30.4 million tons (Greenpeace Southeast Asia, 2011: online). It is not amazing that industrial wastewater will inevitably be contaminated with these reagents and are often released in water without any further treatments. To avoid water pollution, these compounds need to be removed or degraded before being released to the environment.

Phenol is an organic compound that becomes the most abundant pollutant in industrial wastewater because it is widely used in various manufacturing processes such as dyes, pharmaceuticals, pesticides and solvents. Due to its toxicity, phenol in wastewater needs to be degraded to an acceptable level before it is discharged to the environment. The destruction of phenol by using titanium dioxide (TiO_2) catalyst in photocatalysis process was reported to degrade phenol to harmless end products such as CO_2, H_2O. Nevertheless, TiO_2 powder has some limitations in recovering and recycling process at industrial scale. Therefore, in this work we are interested in the use of chitosan as a support for TiO_2 to degrade phenol from wastewater and various parameters which effect phenol photodegradation will be studied.

1.1 Phenol

Phenol is one of a number of chemically active compounds which is found throughout nature, especially in plants. Their molecules consist of hydroxyl functional group (OH) bonded to the ring of an aromatic compound — a molecule that includes at least one ring of carbon atoms. The word *phenol* may also refer to carbolic acid (C_6H_5OH) (Figure 1.1), the simplest form of this group of chemicals and heralded the toxicity.

Figure 1.1 Structure of phenol.

Phenol is a white crystalline (at room temperature), odorous and toxic chemical compound which is widely used as a raw material in the manufacture of other chemical products. It is vastly used in the synthesis of dyes, pharmaceuticals, pesticides and solvents (Keith and Telliard, 1979; Rubin et al., 2006; Laoufi et al., 2008). The physical and chemical properties of phenol are shown in Table 1.1. Phenol was originally isolated from coal tar streams, but through technological advances it is now almost entirely produced synthetically. The dominant process in use today is the distillation from petroleum and synthesis by oxidation of cumene (a product of benzene and propylene reaction) and the subsequent cleavage of cumene

hydroperoxide to form phenol and acetone, and by vapor-phase hydrolysis of chlorobenzene (Figure 1.2) (Carey, 2000). In 2004, the total annual capacity of phenol production approached 3 billion kilograms (CMR, 2005).

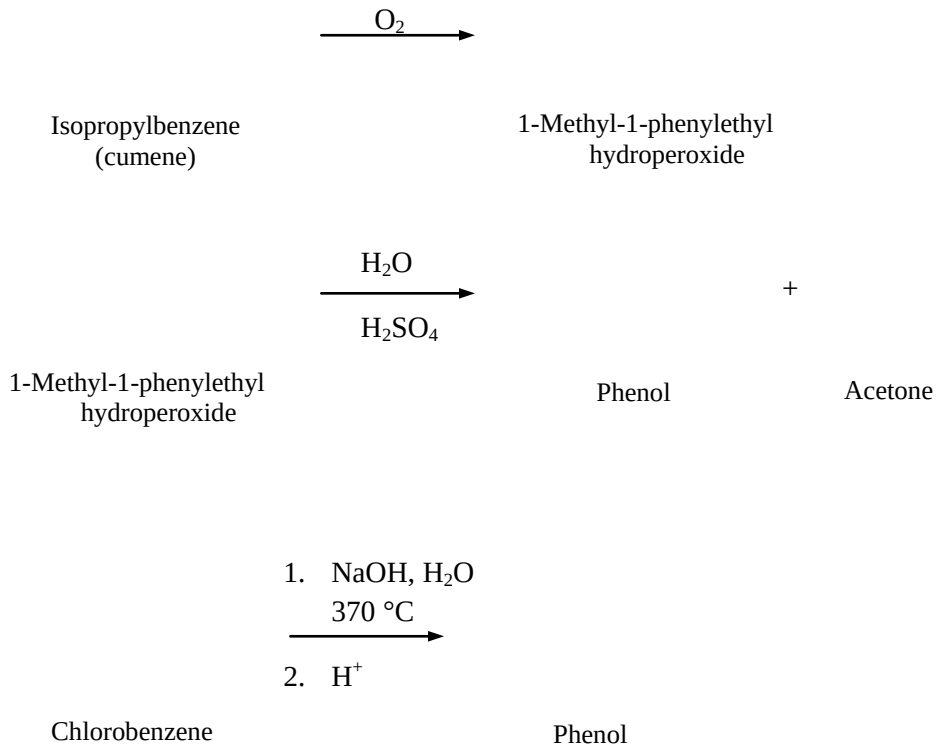

Figure 1.2 Industrial synthesis of phenol (Carey, 2000).

Table 1.1 Physical and chemical properties of phenol (HSDB,2008)

Common synonyms	acidum carbolicum, acidum phenolicum, benzophenol, carbolic acid, hydroxybenzene, monohydroxybenzene, oxybenzene, phenic acid, phenyl hydroxide, phenylic acid, phenylic alcohol
Description	colourless to light pink solid
Molecular formula	C_6H_5OH
Molecular weight	94.11 g/mol
Density	1.0576 g/cm^3 @ 20° C
Boiling point	181.75° C
Melting point	40.9° C
Vapor pressure	0.3513 torr @ 25° C
Odor threshold	40 ppb (150 mg/m^3) (Amoore and Hautala, 1983)
Solubility	86,000 ppm in water, very soluble in alcohol, carbontetrachloride, acetic acid and liquid sulfur dioxide; soluble in chloroform, ethyl ether, carbon disulfide; slightly soluble in benzene
Henry's Law Constant	3.97 x 10^{-7}ATM-m^3/mol (25 °C)
Conversion factor	1 ppm = 3.85 mg/m^3

1.1.1 Phenol toxicity

Phenol is rapidly absorbed following inhalation, ingestion and through the skin. The noxious influence of phenols and their derivatives concerns acute toxicity, histopathological changes, mutagenicity and carcinogenicity (Michałowicz and Duda, 2006). Acute ingestion and skin exposure can cause systemic effects such as anorexia, headache, dark urine, hypothermia, hypotension, arrhythmia and coma. Chronic exposure of phenol may cause skin irritation, inflammation, anorexia, weight loss, salivation, muscle weakness, liver and kidney damage (IRIS, 2002).

1.1.2 Metabolism of phenol (IRIS, 2002)

Phenol metabolic pathway is shown in Figure 1.3. After oral uptake of phenol, the liver, lungs and the gastrointestinal mucosa are the most important sites of phenol metabolism (WHO, 1994). Phenol is directly conjugated with glucuronic acid or sulfate to phenyl glucuronide or phenyl sulphate, respectively. It has been shown to be major metabolic pathways in several species. However, phenol that is not directly conjugated will be a substrate for oxidation reactions. The oxidation products of phenol were hydroquinone and catechols which were generated by the cytochrome P450 2E1 isozyme (CYP2E1), a member of the cytochrome P450 mixed-function oxidase system. These products can be further oxidized by CYP2E1 to trihydroxybenzene or by peroxidation to benzoquinone. Alternatively, the conjugation reactions of hydroquinone or catechol metabolites can occur. In addition, some studies have suggested that biphenols and diphenoquinones can also be produced when peroxidative metabolism of phenol takes place.

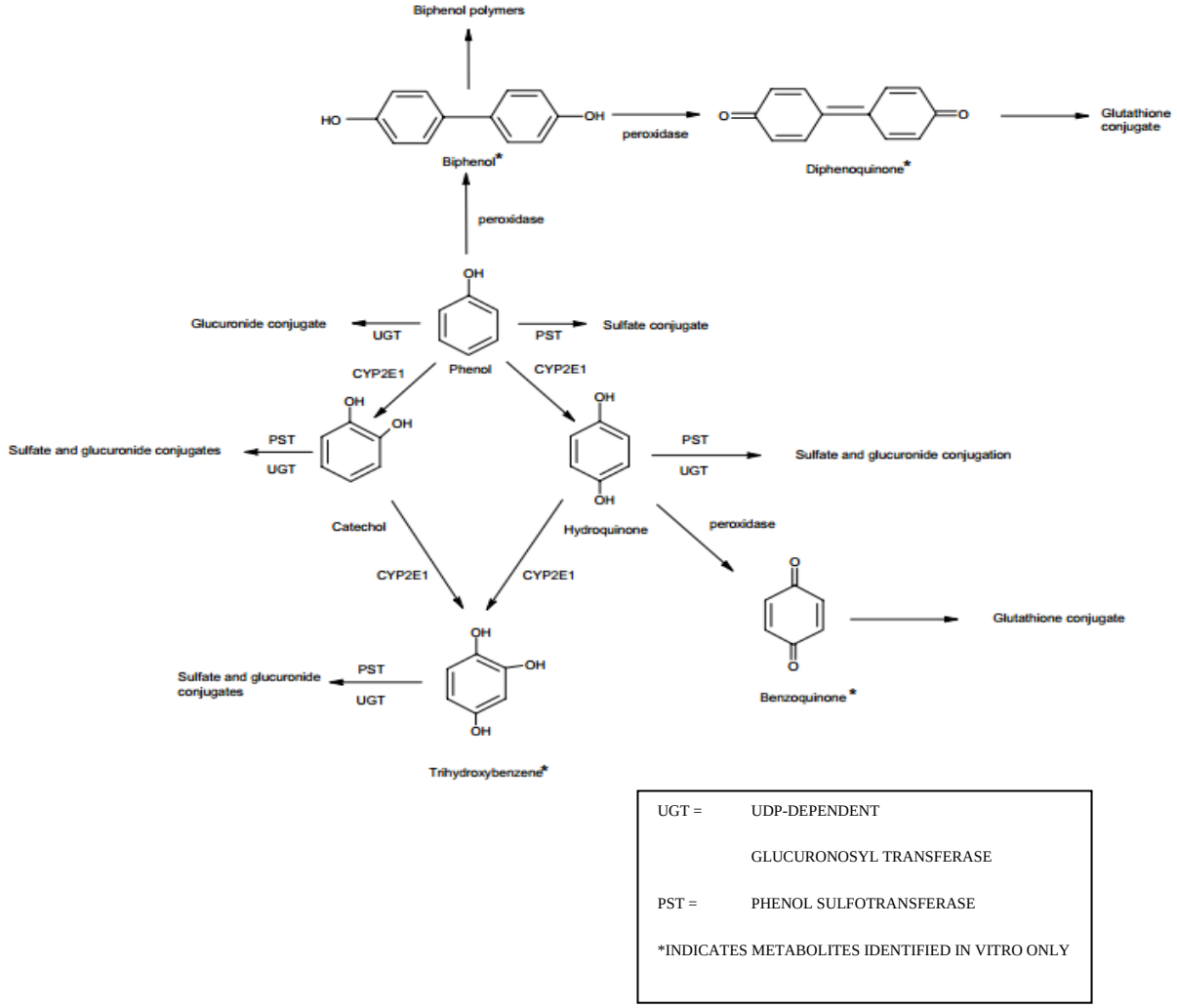

Figure 1.3 Metabolic pathways for phenol (IRIS, 2002).

1.1.3 Phenol treatment methods

Many different treatment methods have been used for the removal of phenol from wastewater, for example microbial degradation (Folsom et al., 1990; Al-Mahin et al., 2010), incineration, solvent extraction (Egorov et al., 2008; Juang et al., 2008), adsorption (Shawabkeh and Abu-Nameh, 2007) and membrane process (Lee et al., 2008; Wu and Li, 2008).

1.1.3.1 Microbial degradation

Phenol is decomposed by microbes such as *Pseudomonas* and *Candida tropicalis* (Al-Mahin et al., 2010). The microbial species possess enzyme systems that are released for the degradation of phenol to harmless end product.

1.1.3.2 Incineration

High concentration of phenol can be eliminated by incineration. The waste is feed to the incinerator with controlling feed rates in order to result in complete combustion. However, before feeding to the furnace, metals, glass and masonry need to be removed to decrease emission of heavy metals from incinerators and limit emission of other pollutants (Environmental and safety services, 1999).

1.1.3.3 Solvent extraction

The extraction solvents for instance cyclohexane, ethyl acetate, chloroform, kerosene and etc. were used to extract phenol from an aqueous solution (Schellin and Popp, 2005). The optimization of extraction conditions such as adjusting the pH-value for the convertion of the compounds into their polar form and the extraction time are necessary. Furthermore, the addition of some compounds will also have to be investigated in order to enhance the extraction process (Khachatryan et al., 2005).

1.1.3.4 Adsorption

There are many adsorbents that have been used for the removal of phenol. Adsorption onto activated carbon is generally used (Tancredi et al., 2004). Recently, polymeric adsorbents for example chitin, chitosan and alginate have extensively been applied as an alternative to activated carbon owing to the cheap cost and adsorption-regeneration properties. Organic pollutants were flown through the column that contained adsorbent or incubated with adsorption materials to remove them from aqueous phase by ionic adsorption. pH, contact time, initial concentration of adsorbents and amount of biosorbent on its adsorption were an important factors for the removal of organic substances (Nadavala et al., 2009).

1.1.3.5 Membrane process

Membrane process has been considered to eliminate some organics pollutants from wastewater. The principle of this method was the use of pressure driven membrane processes for the removal of low molecular weight organic compounds from wastewater (Bódalo et al., 2008). For the removal of phenol, the experiment conditions such as feed phenol concentration, pressure and pH were studied so as to enhance the removal efficiency (Bódalo et al., 2009).

Although the method described above show the capability for the removal of phenol, they have some disadvantages. Despite the use of microorganisms in treatment of phenolic compound in polluted wastewater produce nontoxic end products, the processes for microbial screening, culture and optimize condition finding are difficult and time consuming. Moreover, when the environment changes,

the microbes probably will not be active and may generate secondary toxic intermediates (Busca et al., 2008; Patra and Munichandraiah, 2008).

The air pollution may occur on incineration process. The large quantities of black smoke and the emission of high levels of dioxins were taken place in incomplete combustion which are dangerous to human (Duff, 2006: online).

Solvent extraction, adsorption and membrane process methods are found to be ineffective because they only transfered the organic pollutants from water to another medium without degradation or mineralization of organic pollutants (Thiruvenkatachari et al., 2008).

Recently, a new treatment technology known as a photocatalysis process has been developed. It is capable of the destruction of many organic compounds including phenol to safe end products such as CO_2, H_2O and mineral acid (Qourzal et al., 2006; Shawabkeh et al., 2010).

1.2 Photocatalytic process

Photocatalysis has become an integral part of the advanced oxidation processes (AOPs). Advances in chemical water and wastewater treatment have led to the development of methods termed AOPs or advanced oxidation technologies (AOTs). AOPs can be generally defined as aqueous phase oxidation methods based on the generation of highly reactive species such as hydroxyl radicals (primarily but not exclusively). These procedures may also be combined with ultra sound reactors, UV irradiation and specific catalysts. This results in the generation of hydroxyl radicals in

the mechanisms leading to the degradation of the target pollutant (Vinu and Madras, 2010).

The word photocatalysis is composed of two parts: photo (means light) and the word catalysis (means decompose). It describes a process which light is used to activate a substance, the photocatalyst, which accelerates the rate of chemical reaction without the transformation itself. The photocatalytic reactions may take place homogeneously or heterogeneously. In homogeneous photocatalysis, the reactants and the photocatalysts exist in the same phase. A heterogeneous reaction consists of two phases between a solid photocatalysis (metal or semiconductor) and a fluid containing reactants and products. However, heterogeneous photocatalysis is more studied extensively because it has a potential to be used in various environmental applications. The semiconductors are especially used as photocatalyst due to light absorption properties, charge transport characteristic and exited state lifetime (Kondarides, 2012; online).

Semiconductor photocatalysts (TiO_2, SnO_2, ZnO, WO_3 and etc.) are semiconductors that are able to accelerate chemical reactions on light absorption, typically sunlight (Robertson, 1996). The absorbed photons from the utilizing the energy, photocatalysts can be applied to be used in a wide variety of important chemical processes. Solar fuels production especially hydrogen (H_2) is the ideal fuel for the future because it is clean, energy efficient and renewable energy generated via photocatalytic water splitting over titania and non-titania based photocatalysts (Liao et al., 2012). Environmental remediation also used photocatalyst to destroy many

organic pollutants for air or water purification (Bhatkhande et al, 2001; Yu and Brouwers, 2009).

The molecular orbitals of semiconductors have a band structure. The interested bands in photocatalysis are the occupied valence band and the unoccupied conductance band. They are separated by an energy distance, called the energy band gap (E_g) (Figure 1.4). When the semiconductor is irradiated with light of higher energy than that of the band gap, an electron is promoted from the valence band (VB) to the conduction band (CB) and positive hole (h^+) in the valence band is generated. The electron (e^-) and hole (h^+) pair may recombine with the production of heat. However, they can become involved in electron transfer reactions with other species in the solution if they are separated (Robertson, 1996). The band energy of some semiconductor photocatalysts is shown in Table 1.2.

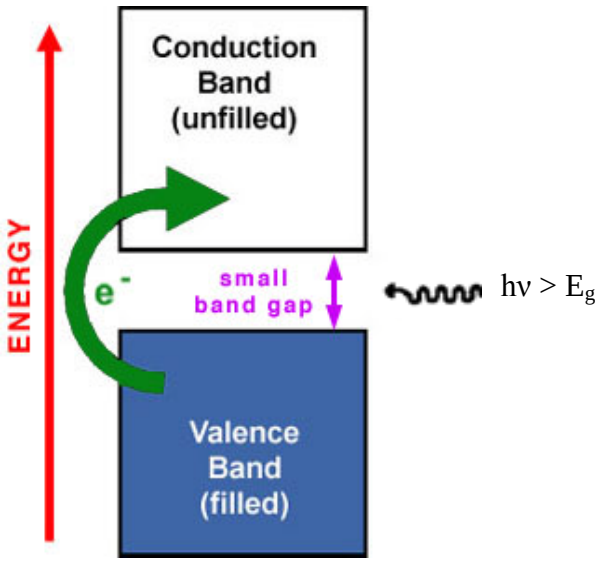

Figure 1.4 In a semiconductor, electrons can be moved from the orbitals in the valence band to the orbitals in the conduction band on illumination.

Table 1.2 The band positions of some semiconductor photocatalysts (Robertson, 1996)

Semiconductor	Valence band (eV)	Conductance band (eV)	Band gap (eV)	Band gap wavelength (nm)
TiO_2	+3.1	-0.1	3.0	380
SnO_2	+4.1	+0.3	3.9	318
ZnO	+3.0	-0.2	3.2	390
ZnS	+1.4	-2.3	3.7	336
WO_3	+3.0	+0.2	2.8	443
CdS	+2.1	-0.4	2.5	497
CdSe	+1.6	-0.1	1.7	730
GaAs	+1.0	-0.4	1.4	887
GaP	+1.3	-1.0	2.3	540

Semiconductors can be used in photocatalysis as particle dispersions or in photoelectrochemical mode. Several hybrid structures have been envisaged to improve photocatalytic performance of semiconductors such as semiconductor-semiconductor or semiconductor-metal and semiconductor-support. The major goals for designing semiconductor–metal composite are to improve the catalytic properties and to enhance the photocatalytic effect in the UV-visible light region (Dawson and Kamat, 2001; Weiss et al., 2001).

The photocatalytic degradation based on oxidation-reduction reaction to exterminate organic pollutant molecules, titanium dioxide (TiO_2) is one of the well known semiconductors that has successfully been used as a photocatalyst because of its high efficiency, non-toxicity, stability, low cost and high activity (Thiruvenkatachari et al., 2008).

1.2.1 Titanium dioxide (TiO_2) photocatalyst

Titanium dioxide (TiO_2) is a semiconductor which shows excellent photocatalyst in various fields. The main advantages of TiO_2 are its photochemical inertness when exposed to acidic and basic compounds, nontoxicity, high oxidizing power and relatively low cost, which make it a competitive candidate for many photocatalysis applications (Castellote and Bengtsson, 2011). Three different crystalline modifications of TiO_2 exist, there are anatase (tetragonal), brookite (orthorhombic) and rutile (tetragonal), the crystal structures are represented in Figure 1.5 (Carp et al., 2004). The anatase form exhibits the highest overall photocatalytic activity. Basic physical properties of the anatase-type TiO_2 are listed in Table 1.3.

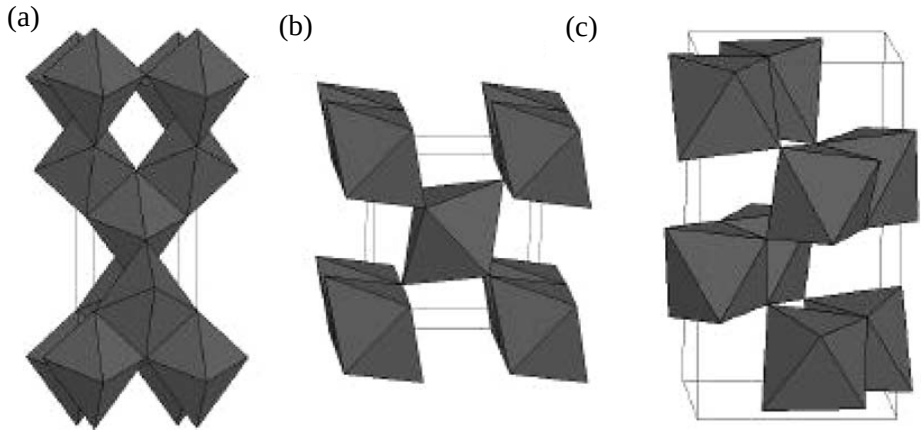

Figure 1.5 The crystal structures of anatase (a), rutile (b), and brookite (c) (Carp et al., 2004).

Table 1.3 Basic physical properties of anatase-type of TiO_2 (Castellote and Bengtsson, 2011)

Crystal form	Tetragonal system
Density (g/cm^3)	3.90
Refractive index	2.52
Permittivity	31
Thermal stability	Change to rutile type at high temperature (~800 °C)

1.2.2 The application of TiO_2

Titanium dioxide is the most widely used white pigment in products such as paints, coatings, plastics, paper, inks, fibres, food and cosmetics because of its brightness and high refractive index (> 2.4) (CERAM Research Ltd, 2002: online). When it is combined with other colours, soft pastel shades can be achieved. Titanium dioxide is allowed to be used at relatively low levels to achieve its technical effect because of the high refractive index that surpassed by few other materials (Hashimoto et al., 2005).

The food applications of titanium dioxide are broad. It is used as colour additive in foods, chewing gum and bubble gum in general at levels not exceed 1%. However, in Japan TiO_2 is used as a food colour without limitation. Besides, TiO_2 is even used in cosmetic and skin care products for example lipsticks, sunblock, soap and body powder (DaNa, 2011: online).

In the environmental applications, environmental remediation includes the degradation, sequestration, or other process approaches, TiO_2 exhibits the benefits for cleanup wastes that results in decreased risks to human and animals by chemical and

radiological contaminants. In 1977, Frank and Bard reported the reduction of CN^- in water by using TiO_2 photocatalysis. It was the first use of TiO_2 for the remediation of pollutants. This has led to a dramatic increase in the research in this area due to the utilization of free solar energy for water and air purification.

Wang et al. (1977) reported the use of TiO_2 surfaces with excellent anti-fogging and self-cleaning abilities. The semiconducting properties of TiO_2 photocatalyst is responsible for the removal of various organic pollutants such as benzene (Einaga et al., 1999), 2,4-dichlorophenol (Trillas et al., 1999; Li et al., 2002), DDT (Quan et al., 2005) and dyes (and Albanis, 2006).

1.2.3 Oxidation-reduction reaction of TiO_2

In photocatalysis, light of energy greater than the band gap of the semiconductor, excites an electron from the valence band (VB) to the conduction band (CB). In the case of anatase TiO_2, the energy band gap is 3.2 eV, therefore UV light ($\lambda \leq 387$ nm) is required. The diagram of photocatalytic degradation is shown in Figure 1.6. An electron (e^-) was excited to the CB when the absorption of a photon occurs to generate a positive hole (h^+) in the VB (eq.1) (Pillai et al., 2012). The e^- and h^+ interact with molecular oxygen that adsorbed on TiO_2 surface to produce superoxide radical anions, $O_2^{\cdot -}$ (eq.2), and with water to yield the highly reactive hydroxyl radicals, HO• (eq.3), respectively. This radical species oxidize a large number of organic substrates to safe end products (eq.4) (Emeline et al., 2001; Horikoshi et al., 2001; Laoufi et al., 2008).

$$TiO_2 + h\nu \longrightarrow e^-_{cb} + h^+_{vb} \quad (1)$$

$$e^-_{cb} + O_2(ads) \longrightarrow O_2^{-\bullet} \quad (2)$$

$$h^+_{vb} + Ti\text{-}OH_2 \longrightarrow HO^\bullet_{ads} + H^+ \quad (3)$$

$$HO^\bullet_{ads} + Pollutant \longrightarrow Photooxidized\cdot product \longrightarrow\longrightarrow\longrightarrow CO_2 + H_2O \quad (4)$$

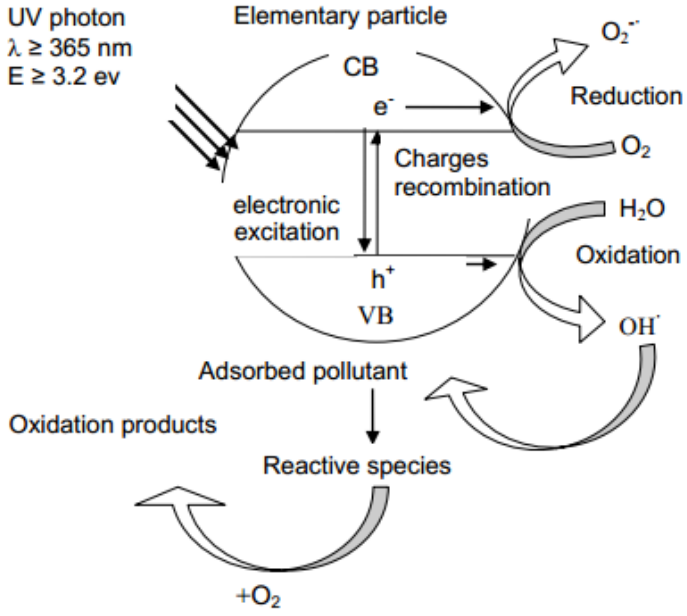

Figure 1.6 Diagram of photocatalytic degradation of TiO_2.

1.3 Phenol destruction by TiO_2 photocatalyst

The intermediates such as catechol, hydroquinone and benzoquinone occurred from the reaction of phenol photocatalytic oxidation in the presence of irradiated TiO_2 were detected (Lupetti et al., 2004). The possible mechanism of the destruction of phenol is shown in Figure 1.7 (Sobczynski et al., 2004). UV illumination of TiO_2 suspension leads to charge carriers (electron (e^-) and hole (h^+)) generated at the surface of the photocatalyst. Photoinduced holes have sufficient oxidizing power to react with hydroxide ions or water molecules producing hydroxyl radicals (•OH). This •OH attacks on the substrate. It has been shown that dihydroxybenzene (catechol, resorcinol and hydroquinone) and *p*-benzoquinone exist in equilibrium solution. It is possible that *p*-benzoquinone can be produced in three different ways: (1) hydroquinone molecule was attacked by •OH, (2) in the reaction of phenol molecule with holes photogenerated in TiO_2 and (3) hydroquinone was directly oxidized by oxygen dissolved in water. Moreover, hydroquinone can be hydrated further to create glycerin and ethanedial. However, 40% of *p*-benzoquinone solution has a fast oxidation in the presence of illuminated TiO_2 which can lead directly to oxygen-contained aliphatic compounds with no further hydroxylation of the compound. In addition, about 60% of the compounds were transferred into hydroquinone. Four compounds of aliphatic intermediates including formic and acetic acids in the reaction mixture were detected. CO_2 and H_2O are the harmless end products of the reaction.

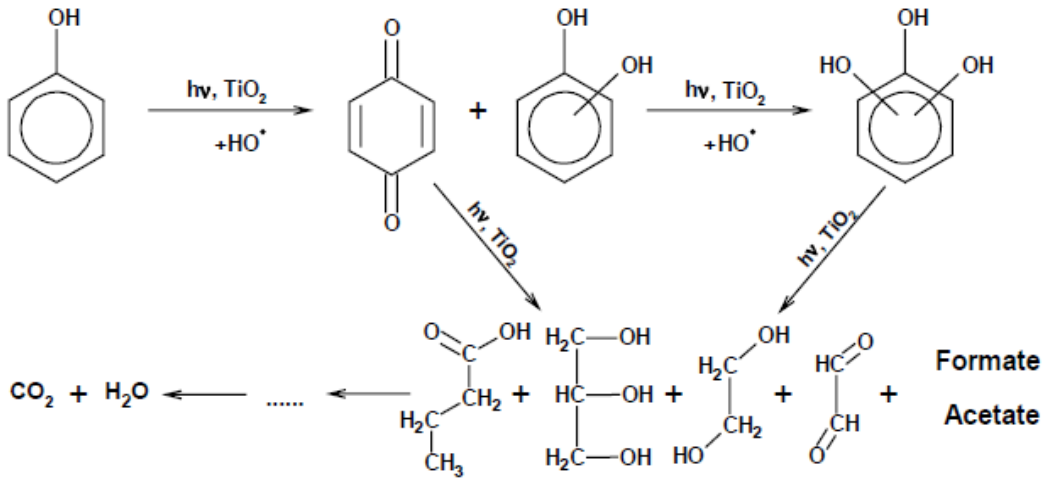

Figure 1.7 The possible mechanism of the destruction of phenol on TiO_2 photocatalyst (Sobczynski et al., 2004).

1.4 Chitosan

In the 21st century, science and technology has moved forward to the renewable raw materials and more environmentally friendly. The natural biopolymer chitin is one of the most common natural polysaccharide after cellulose. Chitosan is the derivative of chitin prepared by the de-*N*-acetylation of chitin which makes up the shells, crabs, shrimp and the cell wall of fungi (Chao et al., 2004).

Chitosan is a natural polymer generally obtained by the deacetylation of chitin which is found in the exoskeletons of shellfish i.e. crab, lobster and shrimp, the cell walls of fungi, cuticles of insects and some algae. Chitosan is a linear polymer of α (1→ 4)-linked 2-amino-2-deoxy-β-D-glucopyranose. It is easily derived by N-deacetylation of chitin and is consequently a copolymer of N-acetylglucosamine and

glucosamine linked by β-(1-4)-glycosidic linkages (Dutta et al., 2004). The structure of chitosan (Figure 1.8) consists of reactive amino and hydroxyl groups that make chitosan very useful in biomedical field and has been found to be highly biocompatible, cosmetic and other applications using its derivative. Chitosan dissolves easily at low pH while it is insoluble at higher pH ranges (Dutta et al., 2004).

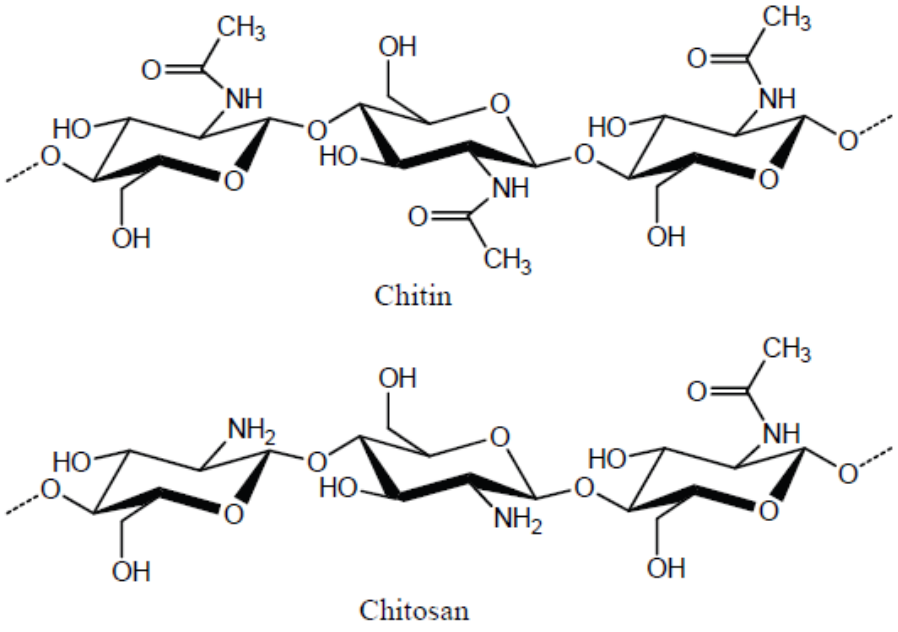

Figure 1.8 Structure of chitin and chitosan.

The degree of deacetylation (%DD) has a significant effect on the solubility and rheological properties of polymer. The degree of deacetylation is one of the most important chemical characteristics of chitosan. Chitosan solubility, biodegradability, reactivity, and adsorption of many substrates depend on the amount of protonated amino groups in the polymeric chain (Rinaudo, 2006). This determines the content of free amino groups in the polysaccharide. Methods for checking the removal of acetyl groups in chitosan include UV spectrophotometry, IR spectrometry, gas chromatography and dye adsorption (Mi et al., 1999). The main attractive force in the development of chitosan is that chitin is the second abundant polymer in nature next to cellulose and thus, more economic. Moreover, chitosan has many beneficial properties such as biocompatibility, biodegradability, hydrophilicity, nontoxicity, anti-bacterial property and high flexibility. For example, they can be formulated into beads, fibers, capsules, powders, gels, membranes, hydrogels and etc. which make chitosan based materials has been applied in food processing, pharmaceutical, agriculture. In addition, chitosan exhibits good adsorption ability for many organic pollutants which has been widely used in the environmental treatment for example, the removal of dye, heavy metals and organic substances (Nawi et al., 2010; Ravi Kumar, 2000; Zheng et al., 2004).

1.4.1 Application of chitosan

1.4.1.1 Food processing

Chitosan has been widely used in food industry because it is non-toxic to human. These biopolymers offer a wide range of unique applications including bioconversion for the production of value-added food products, preservation of foods from microbial deterioration, formation of biodegradable films and clarification and deacidification of fruit juices (Dutta et al., 2004). Other applications of chitosan in food industry are listed in Table 1.4.

1.4.1.2 Cosmetics

Chitosan and hydrophobic substances are compatible with various biologically active components and thus, find a wide application in cosmetics. Chitosan is a natural cationic gum that becomes viscous when mixed with acid which simplifies its interaction with skin covers and hair. It is possible to modify chitosan to chitosan derivatives with varying chain lengths and thus, different properties. For instance, to improve chitosan solubility, the chemical reactions such as acylation, alkylation hydroxyalkylation and carboxyalkylation were employed (Aranaz et al., 2010). In cosmetics the properties operated are bacteriostatic, fungistatic, film-forming, moisture retaining and controlled release of active agent. Some of the applications mentioned in cosmetics are creams, lotions, colour cosmetics (eye shadow, lipstick, make-up, nail polish), shampoo, toothpaste.

Table 1.4 Food applications of chitin, chitosan and their derivatives (Shahidi et al., 1999)

Area of application	**Example**
Antimicrobial agent	Bactericidal
	Fungicidal
	Measure of mold contamination in agricultural commodities
Edible film industry	Controlled moisture transfer between food and surrounding environment
	Controlled release of antimicrobial substances
	Controlled release of antioxidants
	Controlled release of nutrients, flavours and drugs
	Reduction of oxygen partial pressure
	Controlled rate of respiration
	Controlled enzymatic browning in fruits
	Reverse osmosis membranes
Additive	Clarification and deacidification of fruits and beverages
	Natural flavor extender
	Texture controlling agent
	Emulsifying agent
	Food mimetic
	Thickening and stabilizing agent
	Colour stabilization
Etc.	

1.4.1.3 Agriculture

Chitosan has many potential applications in agriculture because the polymer is essentially naturally occurring and biodegradable. Therefore, it should not cause any pollution problems. Chitosan is found to accelerate and enhance growth. Chitosan can be used as seed coating because it has many beneficial effects, such as inhibition of fungal pathogens in the vicinity of the seeds and addition of potting mixture/soil and enhancement of plant-resistant response against diseases (Tseng, 2009: online).

1.4.1.4 Pharmaceutical and biomedical

Chitosan have demonstrated their effectiveness for all forms of dressings-artificial skin, bandages and sponges for surgical treatment because its biocompatibility with human body tissue (Tseng, 2009: online). Chitosan is an excellent medium for reducing side effect, to be used in direct tablet compression, as a tablet disintegrant for the production of controlled release solid dosage forms or for the improvement of drug dissolution (Ravi Kumar, 2000).

1.4.1.5 Wastewater treatment

The biopolymer chitosan can be used as an effective flocculating agent for organic compounds, as a chelating agent and toxic heavy metals trapper, as well as an adsorption medium for dyes and small concentrations of petroleum product, phenols, PCBs and etc. present in various industrial wastewaters. In addition, the amino groups in chitosan are reactive functional groups that can be altered chemically for the production of other chitinous derivatives with specific useful characteristics, for example, as effective absorptive agents. Chitosan exhibiting different physicochemical characteristics, i.e., molecular weight, crystallinity, deacetylation,

particle size, and hydrophilicity, differ in their effectiveness as waste treatment agents. Regenerated chitosan and other chitinous membranes could be broadly used for osmosis, reverse osmosis, micro-filtration, desalination and dialysis (No and Meyers, 2000**;** Dutta et al., 2004). Moreover, chitosan acts as a support for enzyme immobilization and for other catalysts in order to degrade various organic pollutants from wastewater.

Shao and coworkers (2007) studied the immobilization of polyphenol oxidase (PPO) on cross-linked chitosan–SiO_2 gel for treating phenol solution. The efficiency for the removal of phenol (10 mg phenol/L) by the immobilized PPO was 86%, and retained about 60% removal efficiency after five recycles. The enzyme was stabilized with 73 and 58% retention of activity after 10 and 20 days, respectively, at 30°C under optimized conditions.

There are many researchers focused on the use of chitosan and TiO_2 for environmental treatment including Zainal and coworkers (2009). They suggested the newly explored TiO_2–Chitosan/Glass as an alternative material via photodegradation-adsorption process for wastewater treatment. Approximately, 87% of total methyl orange was removed when four layers of TiO_2–chitosan/glass photocatalyst was used. This research work suggested a new method having an advantage of photodegradation–adsorption process in order to reduce various wastewater pollutants.

Liu and coworker (2010) prepared chitosan/activated fiber/TiO_2 membrane to remove 2,4-dichlorophenol (2,4-DCP). The results showed that the lower the initial concentration of 2,4-DCP, the higher the removal rate of 2,4-DCP from aqueous

solution by this material. It can be regenerated up to six cycles by UV-photocatalytic degradation process with 90% efficiency.

Nawi and coworker (2011) immobilized the mixture of TiO_2 and chitosan onto a glass plate for phenol removal. The results showed that the reduction rate by the bilayer TiO_2/chitosan system was faster than the TiO_2 single layer system and slightly better than the TiO_2 powder used in a slurry mode. The adsorption effect of chitosan was negligible and the photodegradation of phenol was largely due to the photocatalytic performance. It represented a good alternative for mineralization of organic pollutants in wastewater.

Chitosan biopolymer has exhibited multifunctional operation with TiO_2 in heterogeneous photocatalysis technology. It is used as a stabilizer, a recovery agent, for enhancing the adsorption capacity of chitosan-TiO_2 adsorbent in the removal of metal ions and for increasing the adsorption-photocatalytic process of the dye species and organic pollutants. Therefore, in this research some alternative materials for wastewater treatment were prepared. We mainly focused on the use of chitosan as a binder and recovered agent for TiO_2 potocatalyst in phenol photodegradation process.

1.5 The objectives of this research

The aim of this study was to prepare three types of Chitosan-TiO_2/TiO_2 beads and to study their photocatalytic activity towards phenol.

1.6 The scopes of research

The scopes of this work were as follows:

1. Preparation of chitosan-TiO_2 beads where chitosan acted as an entrapped agent.
2. Preparation of TiO_2 beads where chitosan acted as a binder.
3. Preparation of modified of TiO_2 grafted chitosan beads.
4. Characterization of obtained beads by using SEM, IR and XRD.
5. Study for their photocatalytic degradation of phenol.
6. Selection for the best bead and optimization for the photocatalytic degradation of phenol.
7. Study of the reusability of the selected bead for the removal of phenol.

1.7 Obtained results

This research provides valuable information on the preparation of beads from chitosan and TiO_2 for phenol photocatalytic degradation which can be further applied for industrial wastewater treatment.

CHAPTER II

MATERIALS AND METHODS

2.1 Materials

- Titanium dioxide powder (The sun chemical Co., LTD, Thailand)
- Chitosan with MW 200-250 kDa and a degree of deacetylation (DD) of 85% (Biolife, Thailand)

2.2 Chemicals

- Phenol (Carlo Erba Reagents)
- Glacial Acetic acid (Carlo Erba Reagents)
- Methanol (Merck, Germany)
- Hydrochloric acid (Carlo Erba Reagents)
- Sodium hydroxide (Carlo Erba Reagents)
- Ethanol, commercial grade
- Ethanol (Carlo Erba Reagents)
- Paraffin oil (Carlo Erba Reagents)
- Petroleum ether 35-60 °C (Mallinckrodt Chemicals)
- Tween 80 (Acros Organics)
- Glutaraldehyde 25 wt% (Acros Organics)
- Acetone (Carlo Erba Reagents)
- Titanium tetraisopropxide 99+% (Acros Organics)
- 3-minopropyl trietoxysilane 99% (Acros Organics)

- 4-aminoantipyrine, reagent grade (Sigma Aldrich, USA)
- Potassium ferricyanide, analytical grade (Analar)

2.3 Instruments

Syringe pump (NE-300, New Era Pump Systems)

Analytical balance (AG204, Mettler Toledo)

Scanning electron microscope (XL30CP, Philips)

Micropipette (100-10000 μl) (Volumate, Mettler Toledo)

Micropipette (1-5 ml) (Volumate, Mettler Toledo)

pH-meter Thermo (Orion* 2 star, Fisher Scientific)

Magnetic stirrer (HTS-1003, LMS)

UV-VIS Spectrophotometer (8453(G1103A), Agilent)

UV/VIS lamp (G 10 W, Synvania ultraviolet)

Fourier Transform infrared spectroscopy (Spectrum One, Perkin Elmer)

X-ray diffractometer (X'pert PW 3710, Philips)

Stirring motor (RW 20 digital, IKA)

Oven (FED-EED, WTB Binder)

Centrifuge (Centra MP 4R, IEC)

Bench Furnace (201 comtroller, Carbolite)

Filter paper

Syringe

Syringe needle

Aquarium air pump

2.4 Preparation of beads

In this research, various types of beads were prepared in order to find appropriate type of beads for the removal of phenol.

2.4.1 Preparation of chitosan beads

Chitosan solution was first prepared by dissolving 2%(w/v) of chitosan in 1%(v/v) of acetic acid and filtered. The viscous solution was extruded dropwise using a 26 gauge syringe needle into a beaker containing 10%(w/v) NaOH in 50%(v/v) EtOH solution dissolved in DI water, with a dropping rate of 60 mL/min. Beads were gently stirred for 30 min and washed with DI water until the pH is neutral. The beads were further washed with 250 mL of 50, 75, 100%(v/v) EtOH and acetone, consecutively. The microparticles were dried at room temperature and kept in the oven at 100 ºC for 24 h.

2.4.2 Preparation of chitosan-TiO_2 beads

Two sizes of chitosan-TiO_2 beads were prepared to study for the effect of surface area of the beads for the immobilization of TiO_2. It consisted of beads in the diameter range of 500-600 μm and the diameter range less than 100 μm.

2.4.2.1 Diameter range of 500-700 µm

Chitosan-TiO_2 was prepared by the addition of various concentration of TiO_2 (0.1, 1, 3 and 50% by wt of chitosan) into 2%(w/v) chitosan solution which dissolved in 1%(v/v) of acetic acid. The solution was stirred until it was homogeneous and beads were produced as described in section 2.4.1.

2.4.2.2 Diameter range less than 100 µm

In this study, chitosan-TiO_2 beads were prepared using the suspension crosslinking technique (Denkbas and Odabasi, 1999).

The homogeneous solution of chitosan-TiO_2 at TiO_2 1% by wt of chitosan was added dropwise into the dispersion medium which consisted of 500 mL of paraffin oil and petroleum ether (25/35, v/v) and Tween 80 0.02 mL/mL medium as an emulsifier. During this process, the medium was stirred with a mechanical stirrer at 1000 rpm for 10 min. After that, glutaraldehyde at 0.033 mL/mL medium was added into the dispersion medium and then stirred for 1 h. Then, 0.033 mL/mL medium of glutaraldehyde was added again into the same medium and stirred for 2 h. The microspheres were collected by centrifugation at 3500 rpm, 25 °C for 15 min and washed twice with 100 mL of petroleum ether and twice with 100 mL of acetone. The microspheres were then dried in an oven at 50 ºC for 24 h.

2.4.3 Preparation of TiO_2 spheres

TiO_2 spheres were prepared according to Vega et al., 2011. Titanium tetraisopropoxide ($Ti(OPr)_4$) was used as the precursor of TiO_2. 0.01 mol of $Ti(OPr)_4$ was added to the solution containing ethanol, DI water, and HCl (37%) in the ratio of 1:0.25:0.1 with continuous mixing by stirrer. The mixture was stirred for 2 h at 25 °C. Commercial TiO_2 powder (5%wt of $Ti(OPr)_4$) which was used as the filler material was added to the clear sol and the solution was stirred vigorously with magnetic stirring. The homogeneous solution was then added to the 3%(w/v) of chitosan solution and then stirred for 30 min. Sphere formation was produced as described under section 2.4.1. Finally, the spheres were dried at 80 ºC for 20 h in the oven and calcined in the furnace at 600 ºC for 3 h to remove the remaining chitosan. This type of beads, chitosan acted as a binder in order to make spheres before it was removed.

2.4.4 Preparation of modified TiO_2 grafted chitosan beads

2.4.4.1 Modification of TiO_2 surface

The modified TiO_2 grafted chitosan beads were prepared according to Simi et al., 2009 and Andrzejewska et al., 2004. Four grams of TiO_2 was treated with 4 g NaOH in 100 mL distilled water. The reaction was refluxed at 85 °C for 2 h. After, precipitate was collected, 46.8 mL of 3-aminopropyl trietoxysilane, 140.7 mL of DI water and 46.8 mL of EtOH were added and the pH was adjusted to 1 with concentrated HCl. The reaction was refluxed at 85 °C for 8 h and the precipitate was collected by centrifugation at 4000 rpm, 25 °C for 15 min and washed with EtOH until the pH is neutral. The modified sample was dried at 100 °C overnight in the

oven and ground with mortar. The ground modified sample was mixed with 0.1%(w/v) glutaraldehyde in isopropanol. This medium was stirred using magnetic stirrer for 8 h at 25 °C. Precipitate formed was washed with isopropanol, centrifuge at 4000 rpm, 25 °C for 15 min. The modified sample was dried at 80 °C overnight in the oven.

In this part of the study, concentration of glutaraldehyde 0, 0.1, 1, 2, 3.75, 5 and 10% (w/v) were used. The concentration that gave the best result was selected to study for the effect of glutaraldehyde incubation time. The incubation time (1, 2, 4, 6, 8 and 10 h) of glutaraldehyde with ground modified sample were then investigated.

2.4.4.2 Modified TiO_2 grafted chitosan beads

Various amount of modified TiO_2 (0.01, 0.1, 1, 5 and 10% (w/v)) were dispersed in a mixture of DI water:ethanol (1:9 v/v). The suspensions of modified TiO_2 consisted of various amount of modified TiO_2 in 5 mL of DI water. The mixture was sonicated for 10 min and 45 mL of ethanol was added to give a total volume of 50 mL. The mixture was sonicated again for 20 min. The suspension was then mixed with 30 g of wet chitosan beads from section 2.4.1 and sonicated for 20 min. Modified TiO_2 grafted chitosan beads were washed five times with 100 mL of mixture of DI water:ethanol (1:9 v/v) and dried at 100 °C in the oven overnight. Beads were kept in a vacuum desicator for further study.

2.5 Characterization of beads

2.5.1 Scanning Electron Microscope (SEM)

The morphology of various types of beads was observed by SEM (Phillips, XL30CP). The samples were mounted directly onto the SEM sample holder using double-side sticking tape and were gold spray-coated. Scanning was carried out under high vacuum with electron voltage of 20 kV.

2.5.2 X-ray diffractometer (XRD)

To determine the crystal structure and crystallinity, TiO_2 and modified TiO_2 were investigated by XRD (Rigaku, DMAX) with Cu Kα radiation (λ=0.15406 nm) at a voltage of 40 kV and current of 30 mA. The prepared sample was taken to expose to the x-ray diffraction chamber. The X-ray diffraction patterns were recorded in the 2θ angle range of 5° to 80°.

2.5.3 Fourier Transform Infrared – Attenuated Total Reflectance (FTIR-ATR)

The distinctive functional groups were recognized by FTIR-ARR (Perkin Elmer, Spectrum One). An attenuated total reflection accessory operates by measuring the changes that occur in a totally internally reflected infrared beam when the beam comes into contact with sample directly. The samples were scanned between 4000 and 500 cm^{-1}.

2.6 The photocatalytic experiments

In this work, the photodegradation chamber was designed as shown in Figure 2.1. Two-hundred milliliters of phenol aqueous solution and 0.3-0.5 g of beads were loaded into a beaker and oxygen was flown through the solution using aquarium air pump. The distance between UV lamp and the surface of solution was set at 15 cm in a dark chamber. The beads and the solution were then irradiated under UV lamp (G 10 W, Synvania ultraviolet) for 8 h. At the desire irradiation time interval, 2 mL portions of the solution were sampled. The concentration of phenol was analyzed by colorimetric assay using 4-aminoantipyrine (4-AAP) and potassium ferricyanide ($K_3Fe(CN)_6$). One milliliter of 10 mM 4-AAP in 100 mM carbonate buffer pH 10 and 1 mL of 10 mM $K_3Fe(CN)_6$ in 100 mM carbonate buffer pH 10 were added respectively into 1 mL of phenol sample. The mixture was incubated for 6 min and the absorbance was then read at 510 nm (Wagner and Nicell, 2002). The % reduction of phenol was calculated by the formula:

$$\% \text{ Reduction} = [(C_0-C_t)/C_0]*100$$

Where C_0 and C_t are the initial phenol concentration and the concentration of phenol in solution at a given time.

The distance between UV lamp and the surface of the solution (10, 15, 20 cm), the stir of the solution, modified TiO_2 concentration (0.01, 0.1, 1, 5, 10% (w/v)), temperature (20, 30, 40, 50, 60 °C), light intensity (10, 20, 30 and 40 W) and initial phenol concentration (10, 25, 50 and100 mg/L) were varied, respectively, in order to

investigate the effects of these parameters on phenol degradation. An optimum condition was then chosen for further study.

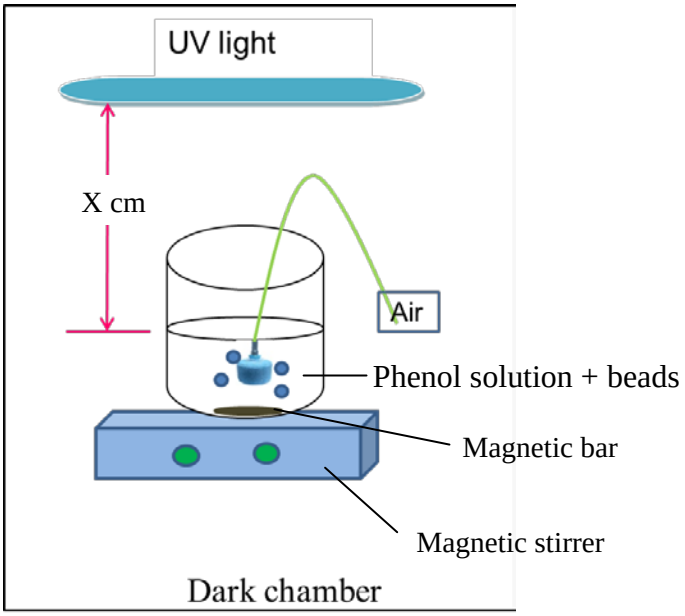

Figure 2.1 Photodegradation chamber for phenol degradation**.**

2.7 Recycling test

For each new cycle, beads were filtered using colander, washed 3 times with 50 mL of DI water and once with 50 mL of EtOH. The beads and the washing solution were shaken by mechanical shaker for 10 min and beads were collected by colander before next washing. The washed beads were then dried in oven at 100 °C before use in the next cycle.

CHAPTER III

RESULTS AND DISCUSSION

In this work, various types of beads were prepared through the use of chitosan as a recovery agent and binder and as a support for TiO_2 photocatalyst in the phenol photodegradation process. The materials were characterized by Scanning Electron Microscope (SEM), X-ray diffractometer (XRD) and Fourier Transform Infrared Spectroscopy (FT-IR). The effects of parameters on phenol photodegradation were investigated.

3.1 Characterization of chitosan-TiO_2 beads

Chitosan-TiO_2 beads were prepared for the photodegradation of phenol. Chitosan solution was mixed with TiO_2 powder and then the beads were produced by dropping into a beaker containing 10%(w/v) NaOH in 50%(v/v) EtOH solution using syringe needle. Chitosan acted as a recovery agent for TiO_2 which was trapped inside chitosan-TiO_2 beads. Chitosan beads without TiO_2 were also prepared and used as a control.

The microstructure of chitosan beads and chitosan-TiO_2 beads were analyzed using Scanning Electron Microscope (SEM). SEM analysis gives the information about the sample's surface, topography and composition. The result is shown in Figure 3.1, both beads had spherical shape with the size range of 500-700 μm and had rather smooth surface.

The beads were then subjected to the Energy-dispersive X-ray spectroscopy (EDX) analysis to investigate what elements were found on the surface of the beads. The result is illustrated in Figure 3.2. It showed that the surface of the chitosan beads and chitosan-TiO_2 beads contained a mixture of C and O which were the main elements of chitosan structure (Larnoy et al., 2011). However, the surface of chitosan beads were contaminated with a small amount of Si and Mg while the surface of chitosan-TiO_2 beads were contaminated with a small amount of Si and Ca. These elements were not the component of chitosan, they maybe spreaded in the air and adhered on the surface of beads. Nevertheless, TiO_2 particles could not be observed on the surface of chitosan-TiO_2 beads. It was presumed that TiO_2 was thus, immobilized in the internal chitosan microsphere.

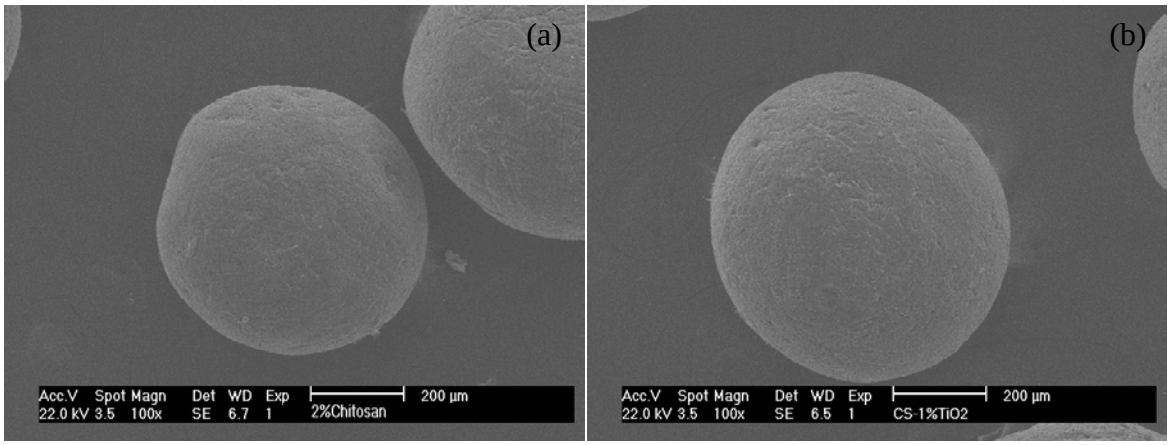

Figure 3.1 SEM picture of 2% (w/v) chitosan in 1% (v/v) acetic acid (a) and chitosan-TiO_2 beads at 1 % of TiO_2 by wt of chitosan (b).

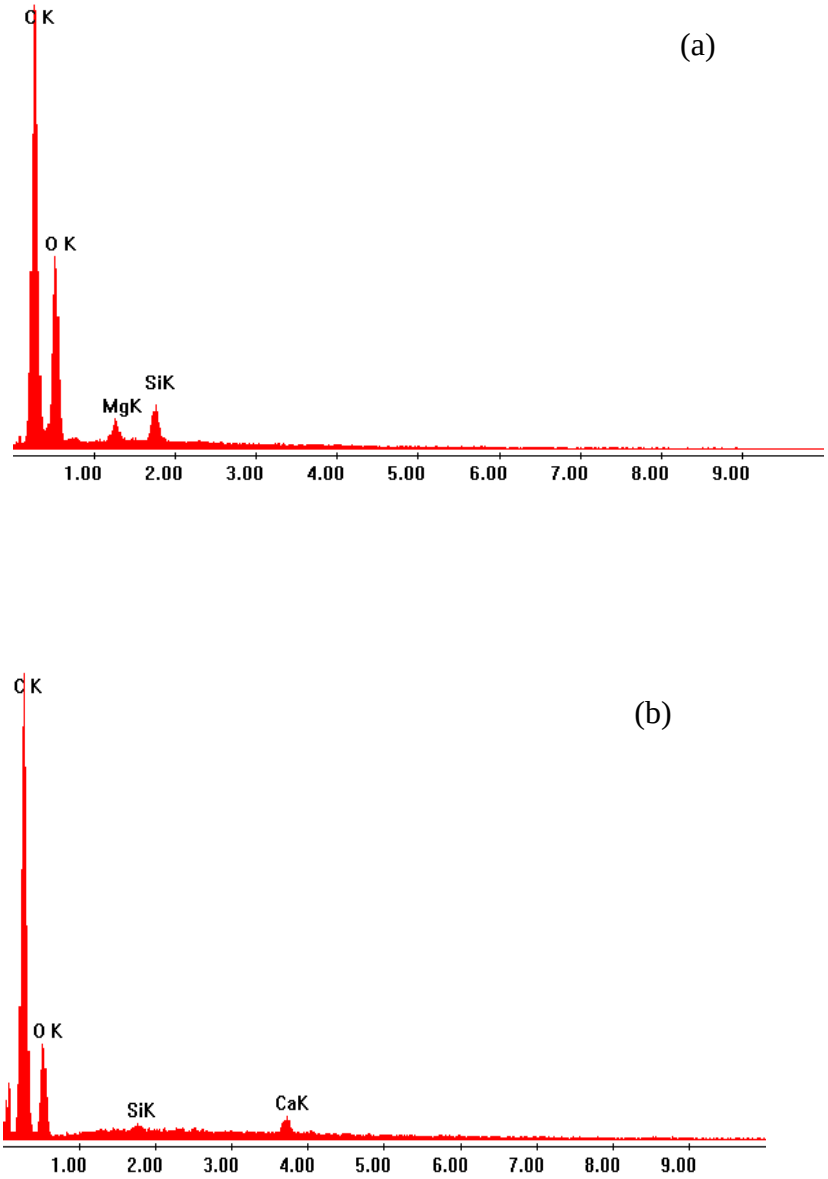

Figure 3.2 EDX pictures of chitosan beads (a) and chitosan-TiO_2 beads (b).

3.2 Phenol photodegradation of chitosan-TiO_2 beads

3.2.1 The effect of TiO_2 dosage of chitosan-TiO_2 beads on phenol photodegradation

Although TiO_2 could not be observed on the surface of chitosan-TiO_2 beads, they were tested for the removal of phenol by photodegradation process.

The dosage of TiO_2 is an important parameter in photocatalytic degradation process. To determine the optimum dosage of photocatalyst, various amount of TiO_2; 0, 0.1, 1, 3 and 50% wt of TiO_2 to chitosan) was prepared. 0.5 g of beads was mixed with 10 mg/L of 500 mL phenol solution. The % reduction of phenol at desired time was calculated (see Appendix A) and plot against reaction time. It can be seen from Figure 3.3 that the % reduction of phenol in the presence of TiO_2 catalyst after 8 h UV irradiation was higher when compared with the reaction mixture without the TiO_2 photocatalyst. The reduction of phenol using chitosan-TiO_2 beads after 8 h UV irradiation at 0.1, 1, 3 and 50% wt of TiO_2 to chitosan were 28.52, 35.67, 32.81 and 28.95%, respectively while chitosan beads without TiO_2 showed 23.08% reduction of phenol. This could be explained by the fact that chitosan has the adsorption ability to remove several organic pollutants including phenol and phenol also was degraded by photolysis process (Nawi et al., 2011; Wu et al., 2001; Zheng et al., 2004). The presence of chitosan-TiO_2 could remove phenol from 5-13 % higher than the reaction mixture without TiO_2. For some reasons, TiO_2 may not be able to degrade phenol efficiently because TiO_2 was not observed on the chitosan surface and thus, resulting in the shielding by chitosan layer. Moreover, from SEM picture (Figure 3.1),

chitosan-TiO_2 had a spherical shape in the size range of 500-700 μm, the surface area per gram support was maybe too low to react with all of phenol molecules. To enhance the surface area per gram support, the smaller size of the beads were then synthesized. However, chitosan-TiO_2 at 1% wt of chitosan was shown to be the best material for phenol removal in comparison with other TiO_2 concentration. Hence, chitosan-TiO_2 at 1% was chosen to compare the capability on phenol degradation with the chitosan-TiO_2 beads in the diameter range less than 100 μm.

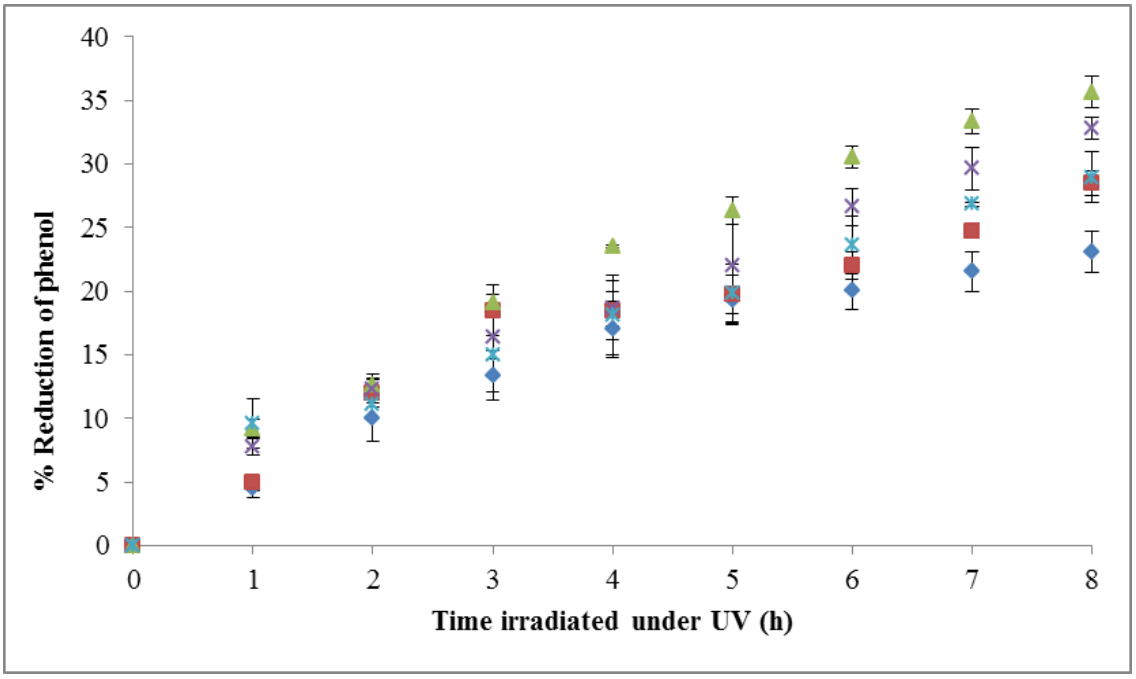

Figure 3.3 Effect of the dosage of TiO_2 catalyst on phenol removal (chitosan beads (◆), chitosan-TiO_2 0.1% (■), chitosan-TiO_2 1% (▲), chitosan-TiO_2 3% (×), chitosan-TiO_2 50% (✳). Condition: chitosan-TiO_2 beads = 0.5 g, initial phenol concentration = 10 mg/L, 500 mL and the distance between UV lamp and the surface of the solution = 15 cm. The error bars represent the standard deviation of three experiments.

3.2.2 Effect of surface area on phenol photodegradation

Chitosan-TiO_2 beads in the diameter range less than 500-700 μm were prepared by water in oil (W/O) suspension crosslinking technique. SEM picture of these beads is presented in Figure 3.4. It can be seen that the beads had spherical shape in the size range of 20-100 μm (Figure 3.4a). Moreover, the surface of the beads was rather rough. The phenol photodegradation of chitosan-TiO_2 beads of both sizes were investigated as previously described. The result (Figure 3.5) indicated that the removal of phenol by the beads in the diameter range of 500-700 μm was higher than the size range of 20-100 μm about 10%. Both types of beads were subsequently subjected to surface area analysis by Brunauer-Emmett-Teller (BET) surface area analyzer method. The chitosan-TiO_2 beads in the diameter range of 20-100 μm showed higher BET surface area (average 4.56 m^2/g) which should facilitate the adsorption of phenol and should enhance the phenol photodegradation than that of the size range of 500-700 μm (1.73 m^2/g). This could be explained by the fact that the medium (paraffin oil and petroleum ether (25/35, v/v)) which was used in W/O emulsification suspension method to produce chitosan-TiO_2 beads in the diameter range 20-100 μm was maybe embedded in the pore of beads. In washing step, paraffin oil could not be washed out completely from the chitosan pore which made it act as a barrier to obstruct phenol adsorption on chitosan and hinder the reaction between UV light and TiO_2 that was contained in chitosan-TiO_2 beads.

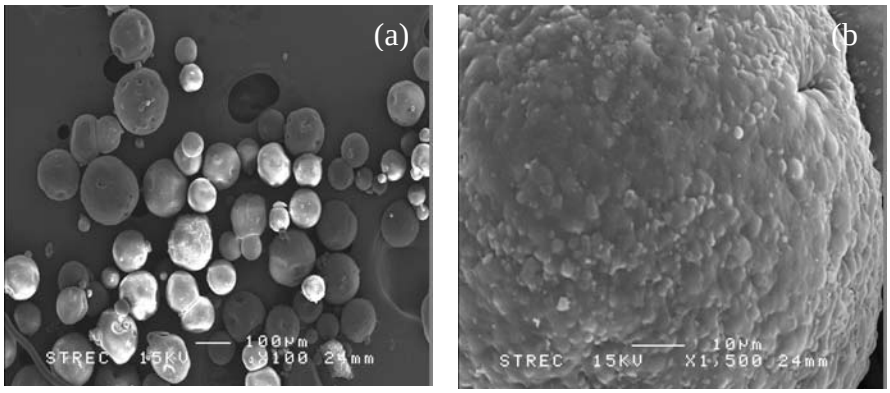

Figure 3.4 SEM picture of chitosan-TiO_2 1.0 % wt chitosan in in the diameter range 20-100 µm at 100X (a) and 1,500X (b).

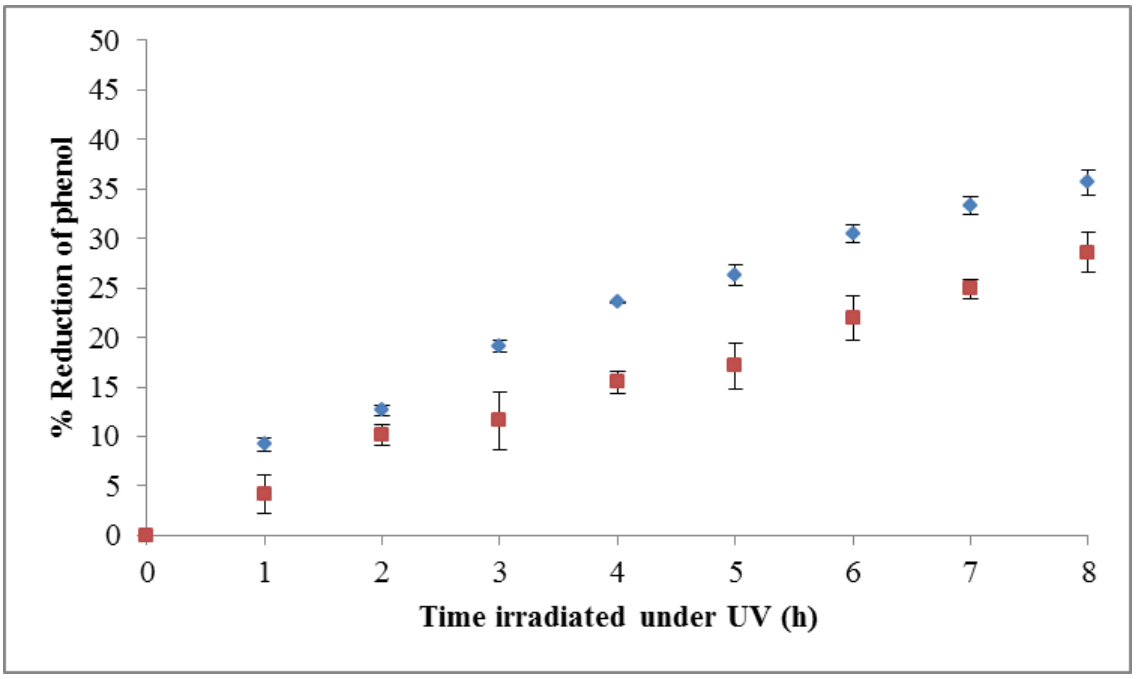

Figure 3.5 Phenol photodegradation of chitosan-TiO_2 beads in the diameter range 500-700 µm (◆) and 20-100 µm (■). Condition: chitosan-TiO_2 beads = 0.5 g, initial phenol concentration = 10 mg/L, 500 mL and the distance between UV lamp and the surface of the solution = 15 cm. The error bars represent the standard deviation of three experiments.

From the results in Figure 3.3 and 3.5, chitosan was used as a recovery agent to store TiO_2 in chitosan beads. The chitosan behaved as a wall to hinder the reaction between TiO_2 and phenol solution. In order to eliminate the negative effect of chitosan, chitosan was then used as a binder to produce TiO_2 spheres. Chitosan solution was mixed with synthetic TiO_2 sol and the beads were formed. After that the spheres were heated at 600 °C to remove any residual chitosan and TiO_2 spheres were generated. The spheres were further characterized and tested for phenol photodegradation.

3.3 Characterization of TiO_2 spheres

TiO_2 spheres had an average diameter of 500-700 µm (Figure 3.6a). When zoomed in the surface of TiO_2 spheres, an assemblage of spherical particles of TiO_2 in varying size ranging from 30 to 300 nm in diameter was observed (Figure 3.6b).

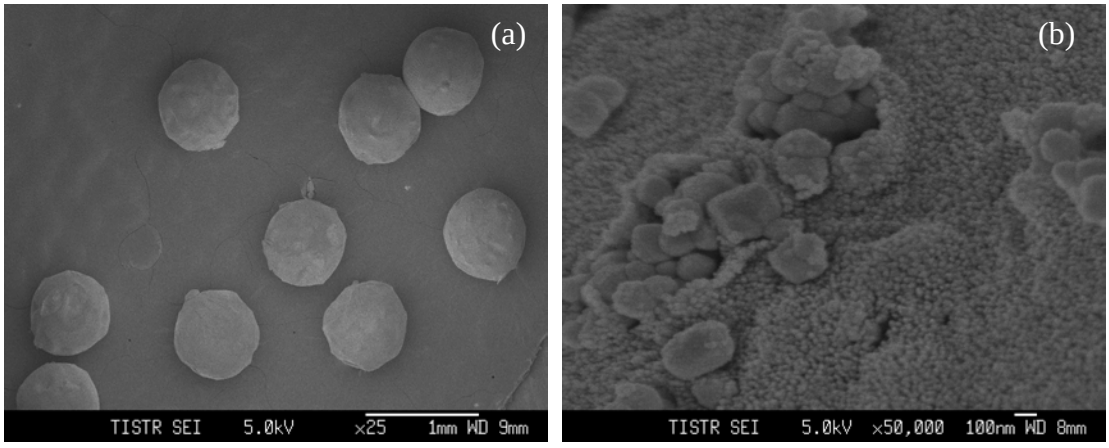

Figure 3.6 SEM images of TiO_2 spheres (a) and the surface of TiO_2 spheres (b).

TiO_2 spheres were then ground and characterized by X-ray diffractometer (XRD) to determine the crystal structure and crystallinity. XRD patterns of commercial TiO_2 powder and ground-TiO_2 sphere are illustrated in Figure 3.7. XRD patterns of commercial TiO_2 which had diameter ranging from 100 to 200 nm showed strong diffraction peaks at 25°, 37° and 48° (Figure 3.7a). These are the characteristics of TiO_2 in anatase form (Thamaphat et al., 2008). The XRD pattern of commercial TiO_2 showed that it is an anatase form which is the most active form of TiO_2. Ground-TiO_2 spheres had diameter ranging from 20 to 50 nm. The diffraction pattern was found to be the same as that of the commercial TiO_2 but lower intensity

was obtained (Figure 3.7b). This could be due the fact that amorphous TiO_2 particles were found. In calcination step, chitosan-TiO_2 sphere were heated at 600 °C to remove chitosan and then TiO_2 spheres were produced. The temperature used for calcination might be too low and thus, an amorphous structure appeared in the sample. It has been shown that an increase in calcined temperatures increased crystallinity of TiO_2 (Wongkaew et al., 2010; Zang et al., 2002).

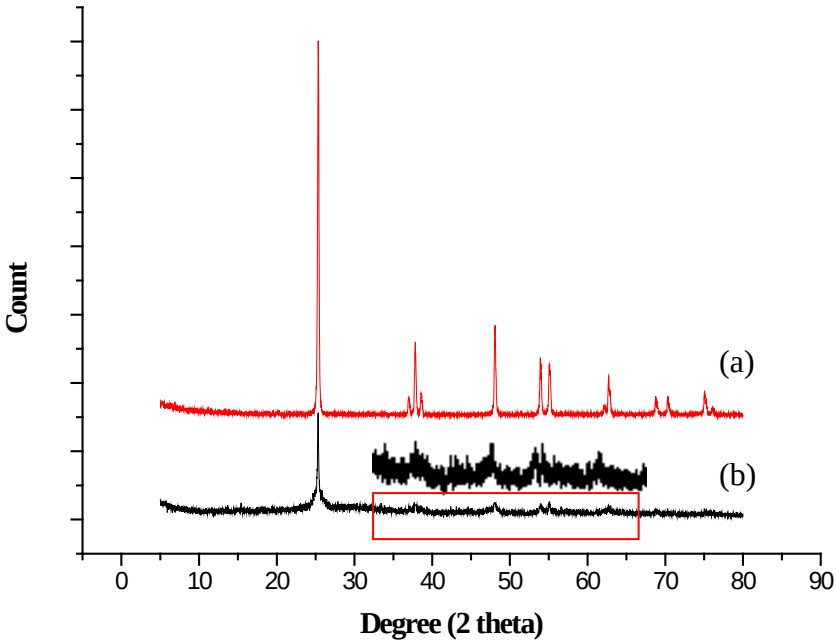

Figure 3.7 X-ray diffraction of TiO_2 powder in anatase form; commercial TiO_2 (a), and ground-TiO_2 sphere (b).

3.4 Phenol photodegradation of TiO_2 spheres

The ability of three types of materials as photocatalysts for the degradation of phenol was investigated. Chitosan-TiO_2 beads at 1.0% wt of chitosan, TiO_2 spheres and commercial TiO_2 powder containing 100 mg of TiO_2 were mixed with 10 mg/L of 500 mL phenol solution. The distance between UV lamp and the surface of solution was set at 15 cm in a dark chamber. The beads and the solution were then irradiated under UV lamp for 8 h. The degradation efficiency of phenol during UV illumination is illustrated in Figure 3.8.

TiO_2 powder was found to be highly photoactive in phenol degradation. After 8 h of UV irradiation, 75% of phenol was degraded. For the degradation of phenol in the presence of chitosan-TiO_2 beads and TiO_2 spheres, 43 and 31% of phenol degradation were observed, respectively. TiO_2 spheres should exhibit better activity for the removal of phenol due to the fact that the surface of TiO_2 spheres contained very small particle size of TiO_2. Hence, they should have high surface area to react with phenol. Furthermore, the effect of chitosan was negligible because chitosan was completely removed by calcination. However, TiO_2 spheres showed the smallest ability for phenol degradation which could be due to the fact that chitosan-TiO_2 beads contained chitosan which had an ability to adsorb phenol. Consequently, chitosan-TiO_2 beads showed higher removal of phenol than that of TiO_2 sphere. In addition, XRD pattern indicated that TiO_2 sphere was in amorphous form which was shown to have lower photocatalytic activity than that of crystalline TiO_2 (Singh and Ghuman, 2012). Moreover, TiO_2 spheres were fragile and tended to break easily when they were mixed with phenol solution which resulting in the difficulty to recover TiO_2 in recovering process.

Therefore, the modification of TiO_2 in order to immobilize it on the surface of the chitosan beads was attempted to improve the efficiency and reusability.

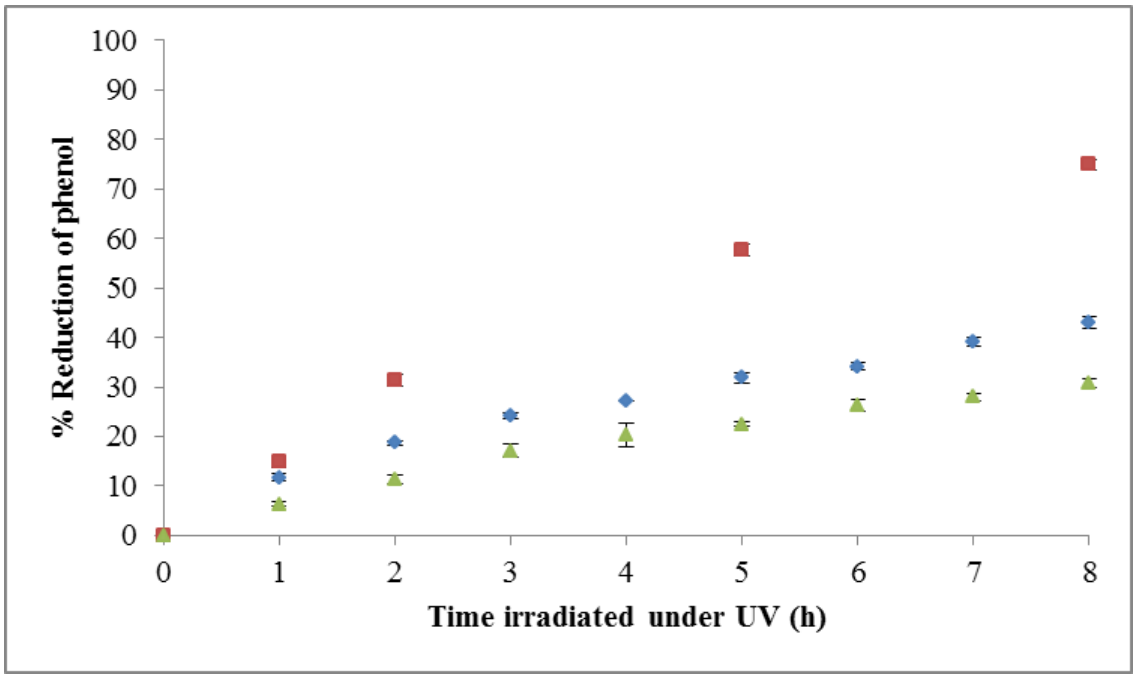

Figure 3.8 The photocatalytic degradation of phenol in the presence TiO_2 powder (■), chitosan-TiO_2 beads in the diameter range 500-700 µm (◆) and TiO_2 spheres (▲). Condition: the amount of TiO_2 in TiO_2 powder, chitosan-TiO_2 beads and TiO_2 spheres = 200 mg, initial phenol concentration = 10 mg/L, 500 mL and the distance between UV lamp and the surface of the solution = 15 cm. The error bars represent the standard deviation of three experiments.

3.5 The Modification of TiO_2 surface

TiO_2 powder was modified which involves two steps. First, TiO_2 was treated with silane coupling agent. They are able to condense with silanol groups of the hydrolyzed silane coupling agent. The reaction mechanism with 3-aminopropyltriethoxysilane can be illustrated as shown in Figure 3.9. At the beginning, aminosilane undertakes hydrolysis with formation of silanol groups:

Figure 3.9 The hydrolysis of 3-aminopropyltriethoxysilane (Andrzejewska et al., 2004).

The condensation with silanol groups on the TiO_2 surface occurs as shown in Figure 3.10.

Figure 3.10 The condensation of TiO_2 with silanol group (Simi and Abraham, 2009).

Then, a Schiff's base formation takes place between the surface of TiO_2 and glutaraldehyde to generate modified TiO_2. Light brown precipitate indicates the formation of Schiff's base with glutaraldehyde. This Schiff's base forms a covalent

bond with NH_2 group of chitosan to produce modified TiO_2 grafted chitosan beads. The scheme of the reaction is presented in Figure 3.11.

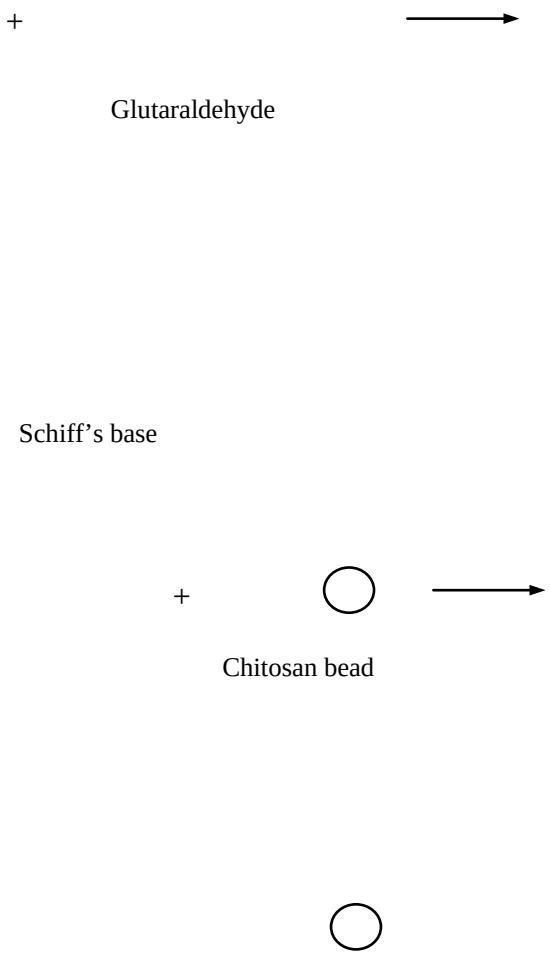

Figure 3.11 Formation of Schiff's base and attachment of TiO_2 to chitosan beads (Simi and Abraham, 2009).

3.6 Characterization of modified TiO_2 and modified TiO_2 grafted chitosan beads

Fourier Transform Infrared – Attenuated Total Reflectance (FTIR-ATR) spectroscopy provides information on the nature of the precursor materials used and the newly synthesized modified TiO_2 grafted chitosan beads catalysts. FTIR-ATR spectra for commercial TiO_2, modified TiO_2, chitosan, and modified TiO_2 grafted chitosan beads are presented in Figure 3.12.

Spectrum peak of TiO_2 should locate at 400-500 cm^{-1} which refers to the vibration of Ti–O bonds in the TiO_2 lattice (Gao et al., 2003; Nur, 2006). Nevertheless it did not appear on the spectrum of TiO_2 in Figure 4.12 due to the limitation of an instrument that can scan only between 4,000 and 500 cm^{-1}.

FTIR-ATR spectrum of modified TiO_2 confirmed desirable linkage of modified TiO_2. Absorption peak at 912 cm^{-1} corresponded to Ti-O-Si bond (Puzenat and Pichat, 2003). The Si-O vibration showed the band at around 1000-1200 cm^{-1} (Siqueira et al., 2007) and the region at 1640 cm^{-1} which attributed to the formation of Schiff's base (C=N bond) (Simi and Abraham, 2009). The peak at 2931 cm^{-1} corresponded to the stretching of C-H group. The band at 3231 cm^{-1} was assigned to OH vibration.

Absorption band of chitosan at 1640 cm^{-1} and 3355cm^{-1} were assigned to its amine (-NH_2) and hydroxyl (-OH) functional groups (Brugnerotto et al., 2001). C-H stretching showed the adsorption band at 2871 cm^{-1}.

FTIR-ATR spectrum of modified TiO_2 grafted chitosan beads showed the combination of chitosan beads and modified TiO_2. When NH_2 of chitosan beads was cross-linked with C=O of modified TiO_2, the Schiff's base peak occurred at 1646 cm^{-1}.

.

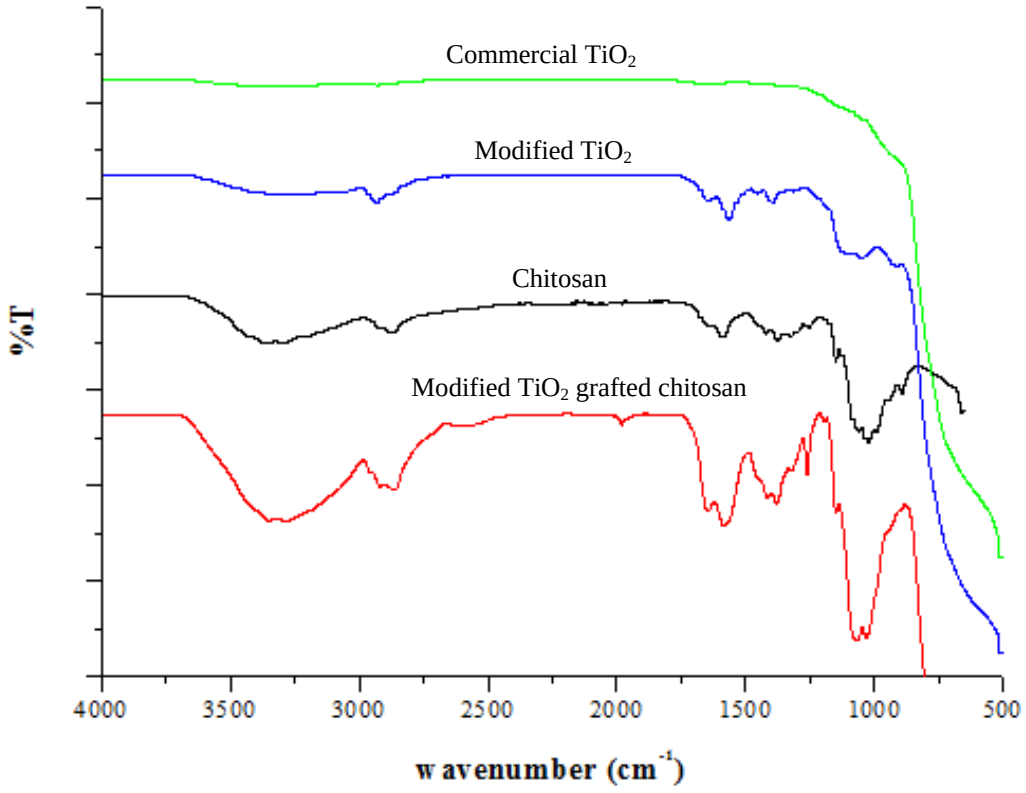

Figure 3.12 FTIR-ATR spectra of TiO_2, modified TiO_2, chitosan and modified TiO_2 grafted chitosan.

The crystalline structure of material was characterized by X-ray diffraction. The X-ray powder diffraction patterns of TiO_2 and modified TiO_2 are shown in Figures 3.13. Both of them represented the peaks at scattering angles of 25.3, 37.8, 48.05 and 62.69° indicating that both preparation of TiO_2 were in anatase phase (Tong et al., 2008). No crystalline phase ascribed to rutile or brookite could be found. This achievement suggested that modified TiO_2 can be used as a photocatalyst in photodegradation process.

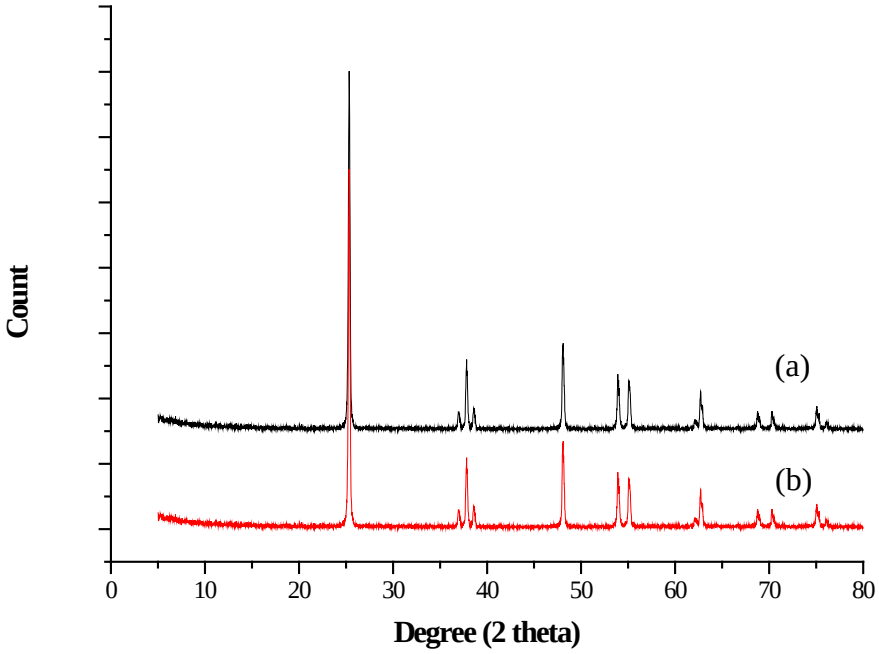

Figure 3.13 X-ray diffractograms of TiO_2 (a) and modified TiO_2 (b).

Next, the modified TiO_2, chitosan beads and modified TiO_2 grafted chitosan beads at 0.01% TiO_2 (w/v) and 1% TiO_2 (w/v) were subjected to SEM analysis (Figure 3.14a-g). The modified TiO_2 had a good dispersion in EtOH:DI water (9:1, v/v). The average diameter of modified TiO_2 particles is 150-200 nm (SemAfore program) as shown in Figure 3.14a. The modified TiO_2 was coated on to the smooth surface of chitosan beads, the thickness of TiO_2 layer depended on the concentration of modified TiO_2. Figure 3.14b, SEM micrograph of modified TiO_2 grafted chitosan beads at 0.01% TiO_2 (w/v) looked the same as that of the chitosan beads without TiO_2 which had smooth surface (Figure 3.14e). However, modified TiO_2 can be observed on the surface of these beads when zoomed in its surface (Figure 3.14c). On the contrary, the agglomeration of modified TiO_2 particles can be clearly seen on the beads at 1% TiO_2 (w/v) of modified TiO_2 and its surface (Figure 3.14f and g). When the bead was broken, the layer of modified TiO_2 that was grafted on the surface of chitosan beads is illustrated in Figure 3.14d and h. The surface of chitosan beads grafting with 1% of modified TiO_2 was found to be thicker than that of chitosan beads grafting with 0.01% TiO_2. The thicker layer was due to the aggregation of modified TiO_2. Modified TiO_2 grafted chitosan beads at 1% TiO_2 (w/v) were then chosen for further study because they can be use in many cycles on phenol photodegradation before the erosion of TiO_2 occurred.

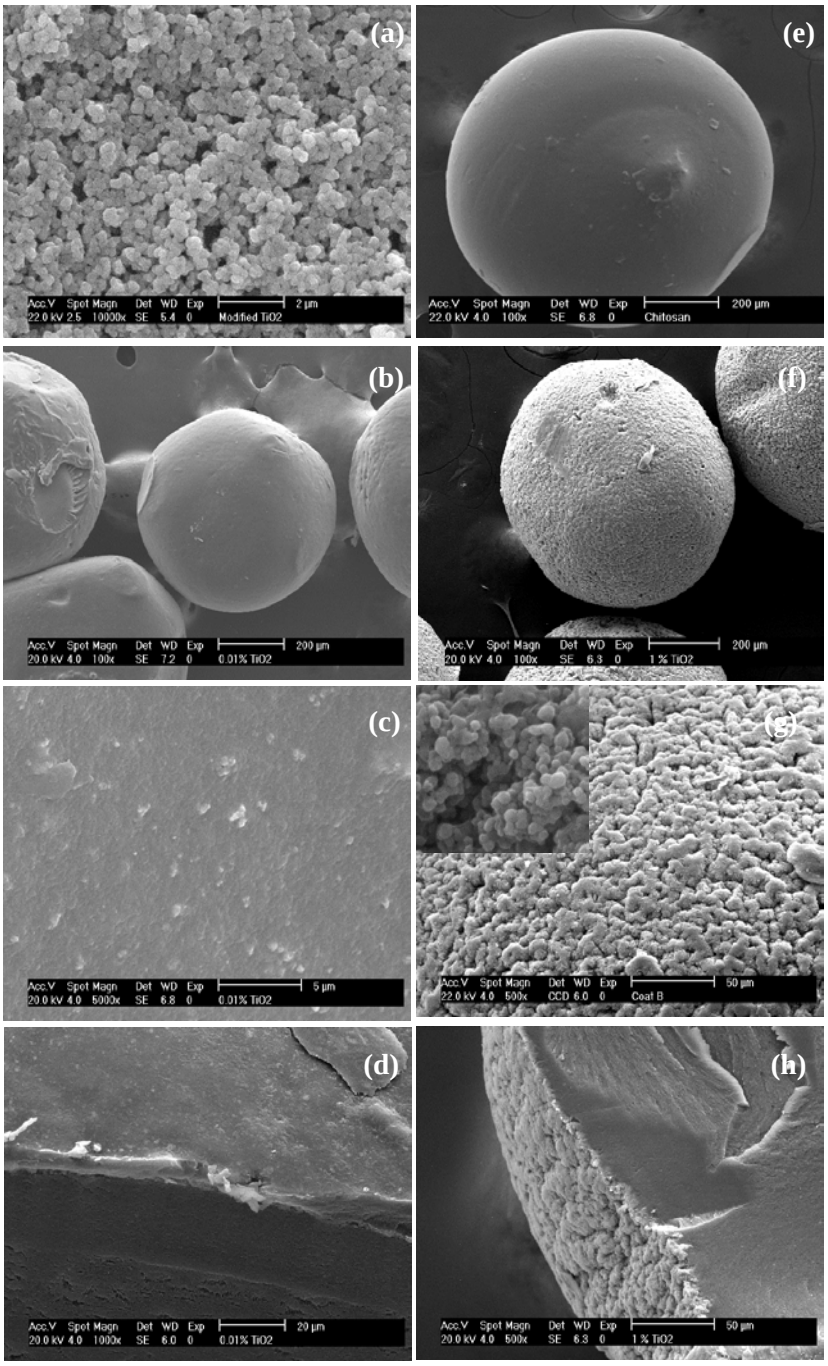

Figure 3.14 SEM pictures of modified TiO_2 (a), modified TiO_2 grafted chitosan beads at 0.01%(w/v) of modified TiO_2 at 100X (b) and 5,000X (c), the broken beads of modified TiO_2 grafted chitosan beads at 0.01%(w/v) of modified TiO_2 (d), chitosan beads (e), modified TiO_2 grafted chitosan beads at 1%(w/v) of modified TiO_2 at 100X (f) and 5,000X (g) and the broken beads of modified TiO_2 grafted chitosan beads at 1%(w/v) of modified TiO_2 (h).

3.7 Phenol photodegradation of modified TiO_2 grafted chitosan beads

3.7.1 Optimization of modified TiO_2 synthesis

The effect of glutaraldehyde concentration and glutaraldehyde incubation time were optimized.

3.7.1.1 Effect of concentration of glutaraldehyde

Glutaraldehyde serves as a cross-linking agent and was used to link the modified TiO_2 on the surface of chitosan beads through primary amine group by Schiff base linkage to produce the layer of modified TiO_2 grafted on chitosan surface. The ground sample which already modified with 3-aminopropyl triethoxysilane was mixed with various concentration of glutaraldehyde (0, 0.1, 1, 2, 3.75, 5 and 10% (w/v)) in isopropanol and incubated at 25 °C for 8 h with agitation using magnetic stirrer. The modified TiO_2 at 1% (w/v) was dispersed in 50 mL EtOH:DI water (9:1, v/v) and coated onto 30 g of wet chitosan beads. Beads were washed five times with the mixture of DI water:ethanol (1:9 v/v) and dried at 100 °C. Three hundred milligrams of modified TiO_2 grafted chitosan beads were loaded into the beaker containing 200 mL of 10 mg/L of phenol and the air was flown through the solution. The distance between UV lamp and the beads was set at 15 cm in a dark chamber. Under UV irradiation, the removal of phenol at several % glutaraldhyde is shown in Figure 3.15.

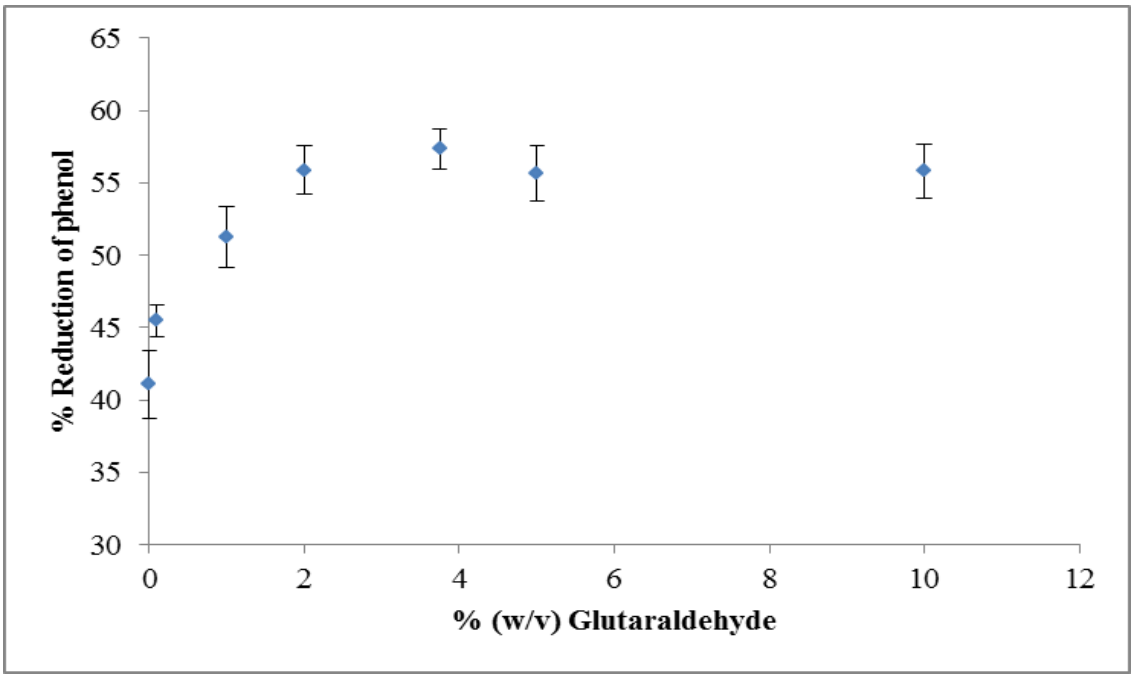

Figure 3.15 Effect of % glutaraldehyde on the removal of phenol at 8 h. Condition: modified TiO_2 grafted chitosan beads = 0.3 g, initial phenol concentration = 10 mg/L, 200 mL and the distance between UV lamp and the surface of the solution = 15 cm. The error bars represent the standard deviation of three experiments.

The removal of phenol was found to increase with increasing amount of glutaraldegyde and reached plateau when glutaraldehyde concentration was higher than 3.75%. This was because of the in excess of glutaraldehyde. Therefore, the concentration of glutaraldehyde at 3.75% was selected for further study.

3.7.1.2 Effect of glutaraldehyde incubation time

Glutaraldehyde at 3.75% (w/v) in isopropanol was added into the ground sample which was modified with 3-aminopropyl triethoxysilane. The incubation time between glutaraldehyde and 3-aminopropyl triethoxysilane at 1, 2, 4, 6, 8, 10 h were studied. Modified TiO_2 at 1% (w/v) was grafted on chitosan beads. Three hundred milligrams of modified TiO_2 grafted chitosan beads were mixed with 200 mL of 10 mg/L of phenol. The beads and the solution were then irradiated under UV lamp for 8 h. The distance between UV lamp and the beads was set at 15 cm in a dark chamber. The % reduction of phenol is represented in Figure 3.16.

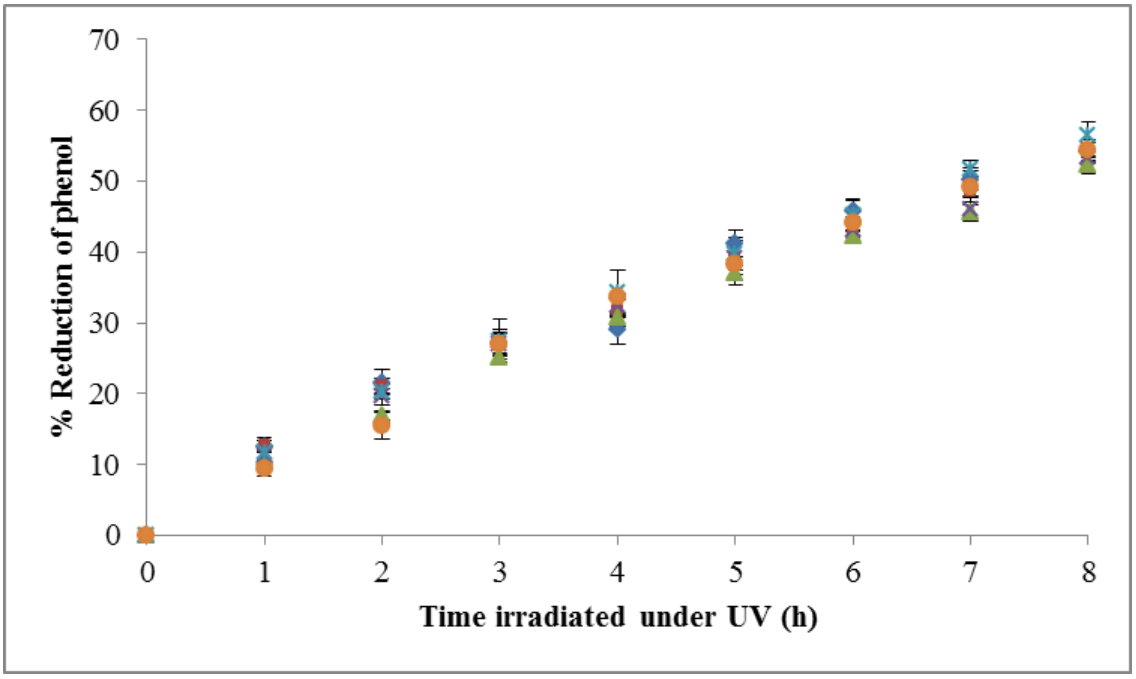

Figure 3.16 Effect of glutaraldehyde incubation time (1 h (◆), 2 h (■), 4 h (▲), 6 h (×), 8 h (✳), 10 h (●)). Condition: modified TiO_2 grafted chitosan beads = 0.3 g, initial phenol concentration = 10 mg/L, 200 mL and the distance between UV lamp and the surface of the solution = 15 cm. The error bars represent the standard deviation of three experiments.

From the result above, the % reduction of phenol from 1 to 8 h of all incubation time of glutaraldehyde was indifferent. It can be seen that the incubation time of glutaraldehyde did not have an effect on the removal of phenol. This could be explained by the fact that the Schiff's base formation between modified TiO_2 and glutaraldehyde (figure 3.17) was already complete at 1 h. So the incubation time at 1 h was chosen for the next experiment.

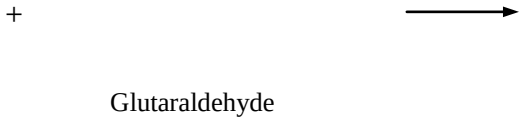

Glutaraldehyde

Schiff's base

Figure 3.17 The formation of Schiff's base between modified TiO_2 and glutaraldehyde.

3.7.2 Effect of parameters on phenol photodegradation

From previous investigation, glutaraldeyde at 3.75% (w/v) was allowed to incubate with modified sample for 1 h. After the modified TiO_2 grafted chitosan beads were prepared, the optimum condition for phenol degradation was studied. Three hundred milligrams of modified TiO_2 grafted chitosan beads were mixed with 200 mL of 10 mg/L phenol solution and the air was flown through the solution. The reaction was set under UV light in the dark chamber.

3.7.2.1 Effect of distance between UV lamp and surface of the solution

The distance between UV lamp and surface of the solution was related to the light intensity (Caimei et al., 2003). This parameter was investigated by changing the vertical distance between the light source and the surface of the phenol solution at 10, 15 and 20 cm. In this experiment, 0.01% (w/v) modified TiO_2 grafted chitosan was used as a photocatalyst.

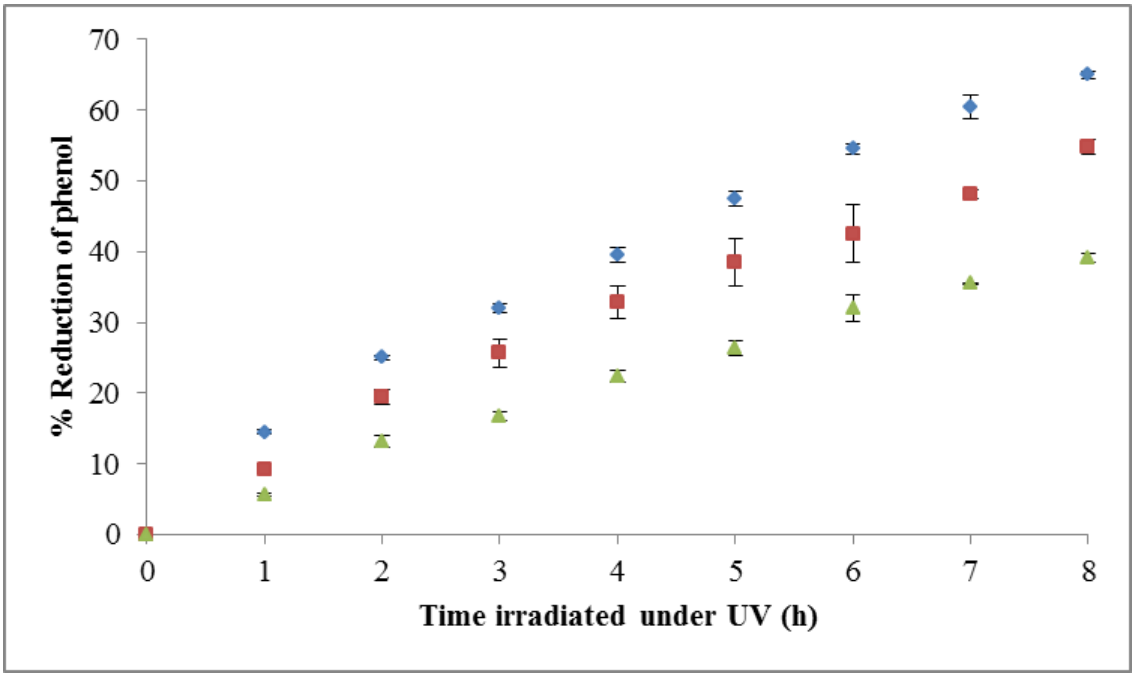

Figure 3.18 Effect of distance between UV lamp and surface of the solution on photocatalysis at 10 cm (◆), 15 cm (■) and 20 cm (▲). Condition: modified TiO_2 grafted chitosan beads at 0.01% (w/v) of modified TiO_2 = 0.3 g, initial phenol concentration = 10 mg/L, 200 mL. The error bars represent the standard deviation of three experiments.

When the distance between the light source and the sample solution increased, the degree of photocatalysis decreased (Figure 3.18) owing to the less intense light used to catalyze phenol by TiO_2. The stronger light intensity led to more photon received by TiO_2 photocatalyst and thus, more $OH^{\cdot}$ radicals were generated to degrade organic pollutant (Caimei et al., 2003). Moreover, the closer distance between the light source and the material could help more phenol molecules react with UV light in photolysis process. Hence, the distance between UV lamp and surface of the solution at 10 cm was selected for the next experiment.

3.7.2.2 Effect of agitation between catalyst and phenol solution

One of the problems in the use of immobilized catalyst for photocatalysis degradation is the limitation in mass transport because the catalyst is immobilized on a solid support (Minsker et al., 2001). From previous experiment, the beads and phenol solution were not thoughly mixed. Only the air flown though the solution that helped the mixing between catalyst and phenol solution. This problem can be overcome by increasing the rate of agitation between the photocatalyst and phenol solution. When the solution was stirred, the beads (0.01% (w/v) of modified TiO_2 grafted chitosan beads) were physically moved all around the solution to enhance its kinetic energy. The beads could then react quickly with photon from UV light and phenol molecule in the solution (Ling et al., 2004). Consequently, the phenol photodegradation increased as shown in Figure 3.19. The reaction without photocatalyst was used as a control which also exhibited the removal of phenol because phenol could be degraded by photolysis process (Nawi et al., 2011; Wu et al., 2001). However, the reaction mixture containing photocatalyst showed higher

% reduction of phenol. Therefore, phenol solution containing modified TiO_2 grafted chitosan beads for all experiments was allowed to stir during photodegradation process.

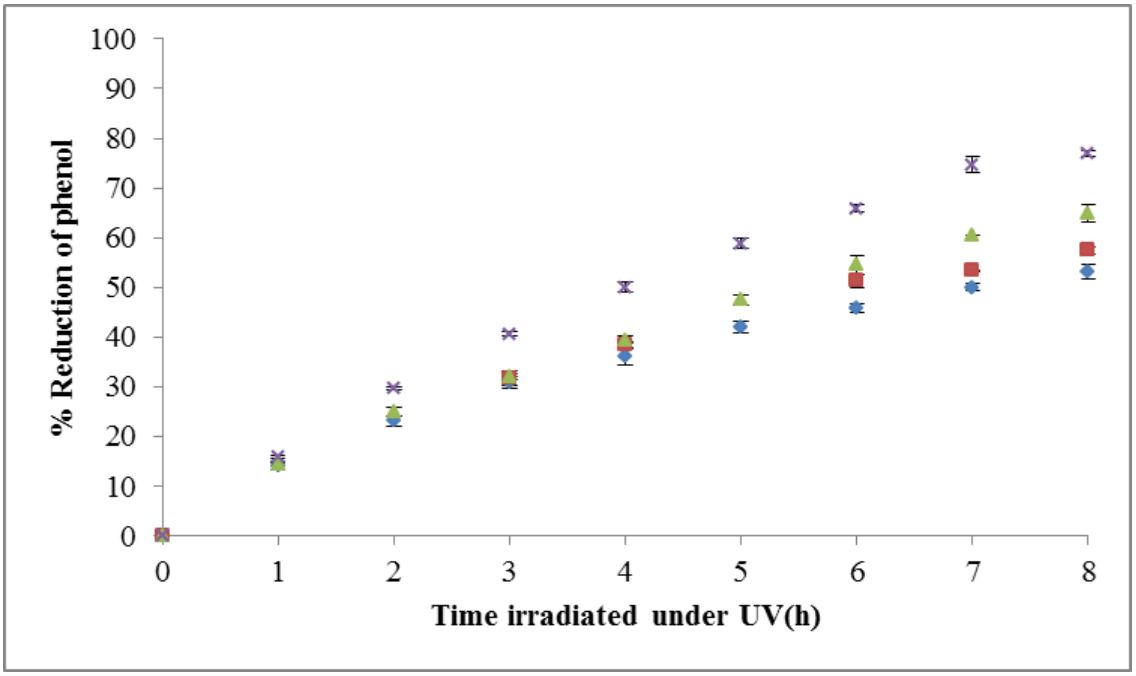

Figure 3.19 Effect of the agitation between phenol solution and TiO_2 grafted chitosan beads on phenol photocatalysis process (0.3 g beads, stirring ( ), 0.3 g beads, no stirring ( ), 0 g beads, stirring ( ), 0 g beads, no stirring ( )). Condition: modified TiO_2 grafted chitosan beads at 0.01% (w/v) of modified TiO_2 = 0.3 g, initial phenol concentration = 10 mg/L, 200 mL and the distance between UV lamp and the surface of the solution = 10 cm. The error bars represent the standard deviation of three experiments.

3.7.2.3 Effect of modified TiO_2 concentration

The modified TiO_2 at 0.01, 0.1, 1, 5 and 10% (w/v) were grafted onto chitosan beads. The removal of phenol is presented in Figure 3.20. The result can be divided into two groups. The first group was the chitosan beads which were coated with modified TiO_2 at 1, 5 and 10% (w/v). These beads showed the reduction of phenol of more than 80% while other modified TiO_2 concentrations (0.01 and 0.1 % TiO_2 (w/v) grafted chitosan beads) represented approximately 75% approximately after 8 h photodegradation. The % reduction after 8 h did not differ much between these two groups. However, during the photocatalysis reaction, the phenol degradation in the first group exhibited approximately 15-30% better phenol removal than the second group. For some reasons, it was found that the outer surface of the grafted beads at 1, 5 and 10% (w/v) of modified TiO_2 were eroded by the stirring process which caused the dispersion of modified TiO_2 powder into the reaction solution. The rate of phenol degradation thus, increased because the UV light could penetrate into the suspension which increased the number of hydroxyl, and superoxide radicals (Laoufi et al., 2008). However, the second group did not erode upon stirring and thus, did not disperse in the solution. The modified TiO_2 grafted chitosan beads of 1% (w/v) of modified TiO_2 were selected for further study because at higher TiO_2 concentration, phenol photodegradation did not increase due to the shielding effect of TiO_2 powder, resulting in erosion and dispersion of TiO_2 in the solution.

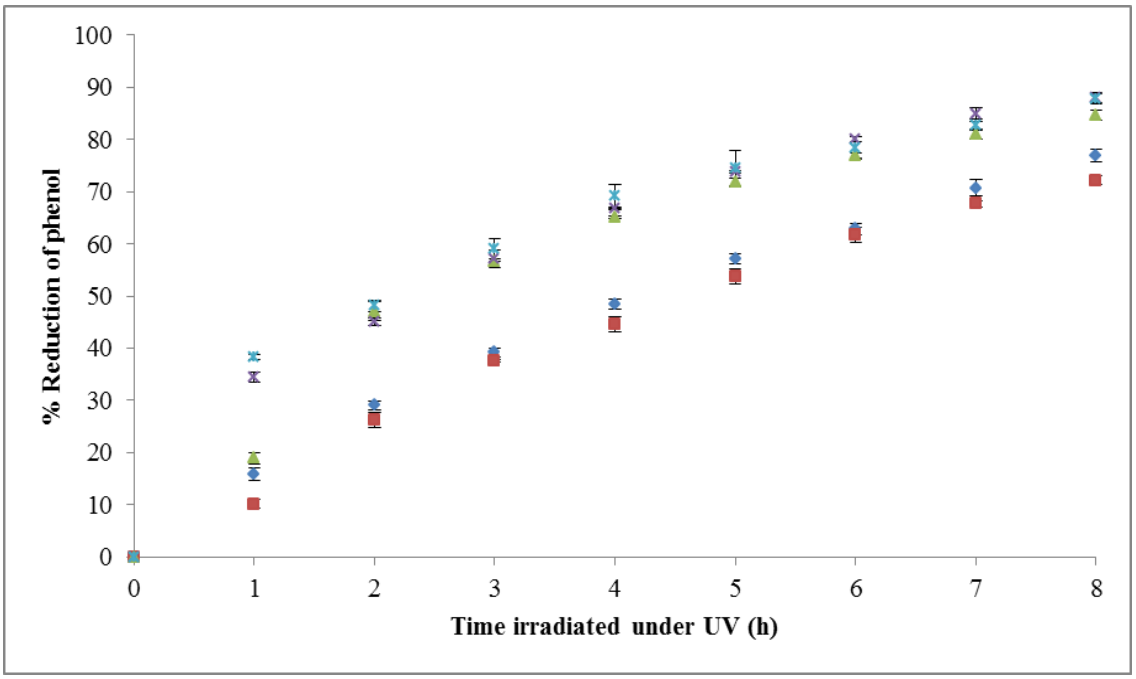

Figure 3.20 Effect of TiO_2 concentration at 0.01% (w/v) (◆), 0.1% (w/v) (■), 1% (w/v) (▲), 5% (w/v) (×) and 10% (w/v) (✳).Condition: modified TiO_2 grafted chitosan beads = 0.3 g, initial phenol concentration = 10 mg/L, 200 mL and the distance between UV lamp, the surface of the solution = 10 cm and stirred reaction mixture. The error bars represent the standard deviation of three experiments.

3.7.2.4 Effect of reaction temperature

To investigate the difference of the reduction of phenol clearly, the photodegadation time at 5 h was used because the degradation reached plateau after 8 h.

Effect of temperature on the degradation of phenol is exhibited in Figure 3.21. As the solution temperature increased, the percent reduction of phenol increased. The degradation rate also enhanced when the temperature was risen up (Figure 3.22). This increase could be explained by the enhancement of the reaction rate took place between the phenol molecules and the hydroxyl radicals. Furthermore, the enlargement of the degradation was presumably due to the increasing collision frequency of phenol molecules (Kim and Lee, 2010). Although the temperature at 60 °C showed the highest phenol degradation, the temperature at 30 to 40 °C was acceptable for the degradation of phenol because it was similar to the environmental temperature. However, temperature at 30 °C was chosen for next study because it used lower electric energy for temperature adjustment.

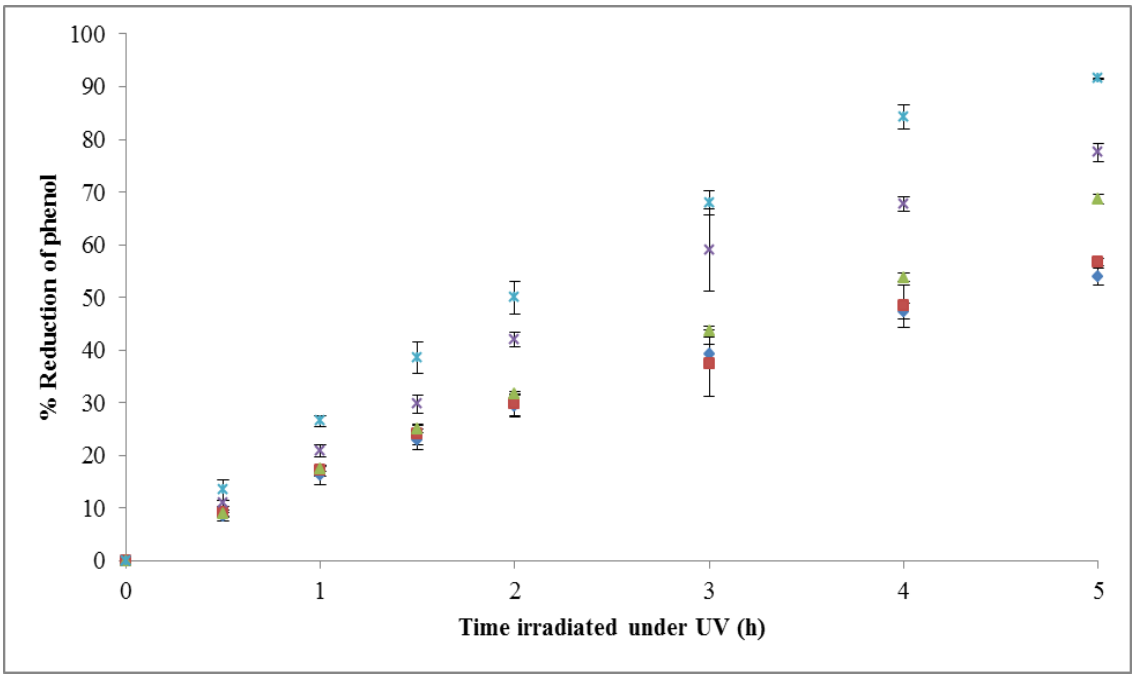

Figure 3.21 Effect of reaction temperature on phenol photocatalytic degradation (20 °C (◆), 30 °C (■), 40 °C (▲), 50 °C (×), 60 °C (✳)). Condition: modified TiO_2 grafted chitosan beads at 1% (w/v) of modified TiO_2 = 0.3 g, initial phenol concentration = 10 mg/L, 200 mL, the surface of the solution = 10 cm and stirred reaction mixture. The error bars represent the standard deviation of three experiments.

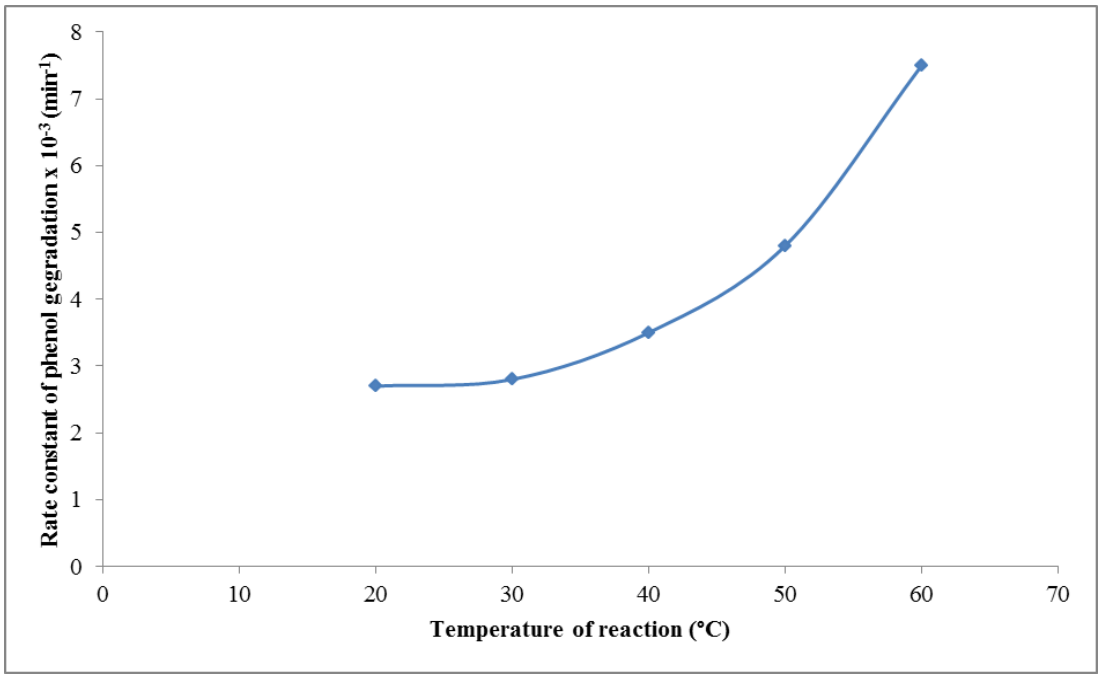

Figure 3.22 The relationship of rate constant vs. reaction temperature at 2 h of degradation time.

3.7.2.5 Effect of light intensity

Intensity of UV radiation has been reported to be an important parameter to control the photoactivity (Lee et al., 2004). In section 3.7.2.1, the distance between UV lamp and surface of the solution which involved light intensity was studied and the distance at 10 cm was chosen for the degradation of phenol. In order to gain higher removal of phenol, light intensity was varied with the fixed distance between UV lamp and surface of the solution at 10 cm. This experiment was conducted under different light intensities of 0, 10, 20, 30 and 40 W by changing the number of lamps which located over the reaction. The results showed that the removal of phenol increased with increasing light intensity as represented in Figure 3.23. The reason was that higher light intensity can produce more photon received by catalyst, resulting in higher generation of e^- and h^+ and then more $OH^\cdot$ radical was created which led to high efficiency of phenol photocatalytic degradation (Lee et al., 2004; Subramanian and Kannan, 2008). In an unirradiated reaction which was used as a control, approximately 15% of phenol was removed due to the adsorption of phenol onto TiO_2 particles and chitosan beads (Laoufi et al., 2008).

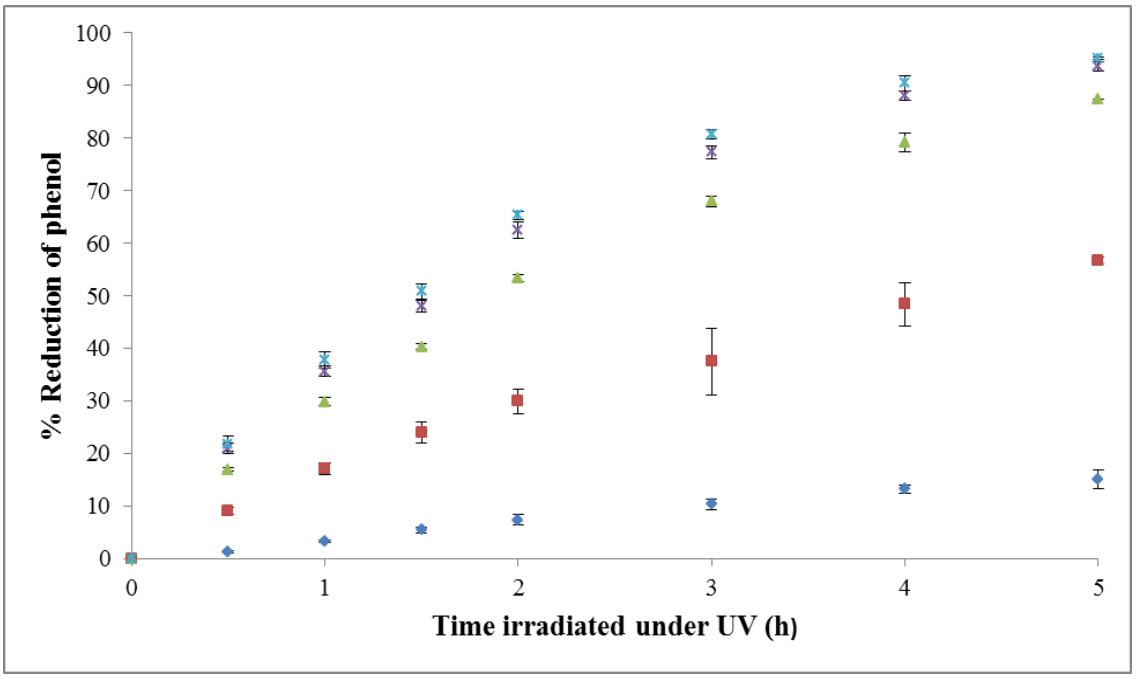

Figure 3.23 Effect of UV light intensity on phenol photogedradation (0 W (◆), 10 W (■), 20 W (▲), 30 W (×), 40 W (✱)). Condition: modified TiO_2 grafted chitosan beads at 1% (w/v) of modified TiO_2 = 0.3 g, initial phenol concentration = 10 mg/L, 200 mL, the surface of the solution = 10 cm, stirred reaction mixture and reaction temperature = 30 °C. The error bars represent the standard deviation of three experiments.

The semilogarithmic plots of concentration was plotted to examine the kinetic order reaction. The data gave a straight line. This finding indicated that the photocatalytic degradation of phenol using modified TiO_2 grafted chitosan beads can be described by the pseudo first-order kinetic model (Mahvi et al., 2007; San et al., 2000) (Figure 3.24) where ln $C_t = -kt$ C+ln C_0 (C_0 is the initial concentration and C_t is the concentration of phenol at time t). The first-order rate constants were estimated (see Appendix B) in Table 3.1.

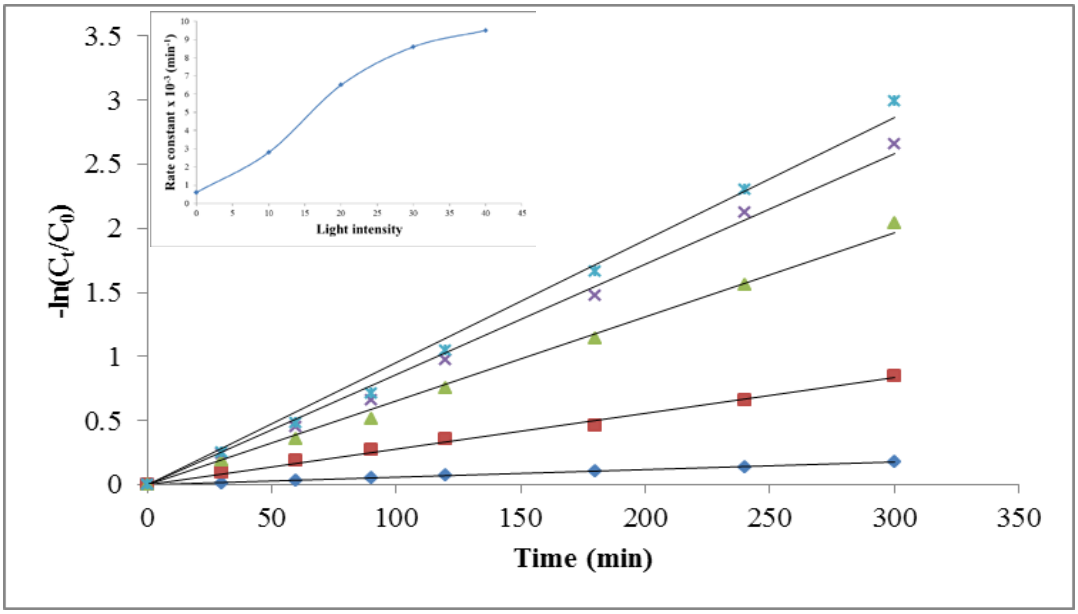

Figure 3.24 Plot of ln C_t/C_0 vs. time for photodegradation of phenol (0 W (◆), 10 W (■), 20 W (▲), 30 W (×), 40 W (✳)).

Table 3.1 First order rate constants for phenol photodegradation at various intensity of UV light

UV light intensity (W)	Rate constant ($x10^{-3}$ min^{-1})	*r*
0	0.6	0.998
10	2.8	0.997
20	6.5	0.998
30	8.6	0.997
40	9.5	0.996

The degradation rate of phenol at 20, 30 and 40 W of light intensity increased 2.3, 3.1 and 3.4 times, respectively when compared with 10 W of light intensity. The rate of phenol degradation when the 40 W-light source was used should have been 4 times higher when compared of that 10 W because the intensity of light was increased 4 times (Lee et al., 2004). This might be due to the fact that the generated light source exceeded the area of beaker containing the reaction solution as shown in Figure 3.25. Thus, some irradiation of UV light did not reach the phenol solution. The light intensity at 20 W was selected for the study on the effect of initial phenol concentration.

Figure 3.25 The UV lamp covered the beaker of phenol solution.

3.7.2.6 Effect of initial phenol concentration

In 2010, Thailand imported phenol for all industrial was of 189,735.58 tons (Pollution Control Department, 2010). The water standard level of phenol in industrial wastewater must not exceed 1.0 mg/L (Pollution Control Department, 2012: online). As the concentration of pollutant is an important factor in wastewater treatment, the initial concentration of phenol was investigated over the range of 10 to 100 mg/L. In order to see the difference of the removal of phenol among various phenol concentration tested, an irradiation time of 2 h was chosen and the result is shown in Figure 3.26. The rate constant *k* together with the correlation coefficients *r* is collected in Table 3.2. The result showed that the rate of photodegradation decreased as the initial phenol concentration increased. This could be explained by the fact that when the initial phenol concentration was extended, the generation of hydroxyl radicals on catalyst surface was reduced due to the adsorption of more phenol molecules and its intermediates on TiO_2 surface (Daneshvar et al., 2005). This caused the lack of active site available for hydroxyl radicals adsorption on the surface of catalyst. Thus, large amount of adsorbed phenol acted as an inhibitor that influenced the reaction between phenol molecules and hydroxyl radicals because they could not contact each other directly (Wong et al., 2011). In addition, the absorption of light by the substrate at high concentrations might intercept the photons before they could reach the photocatalyst surface and hence, the amount of hydroxyl free radical production was reduced (Lam et al., 2010). Besides, the amount of photocatalyst was too low to degrade phenol at high concentration completely.

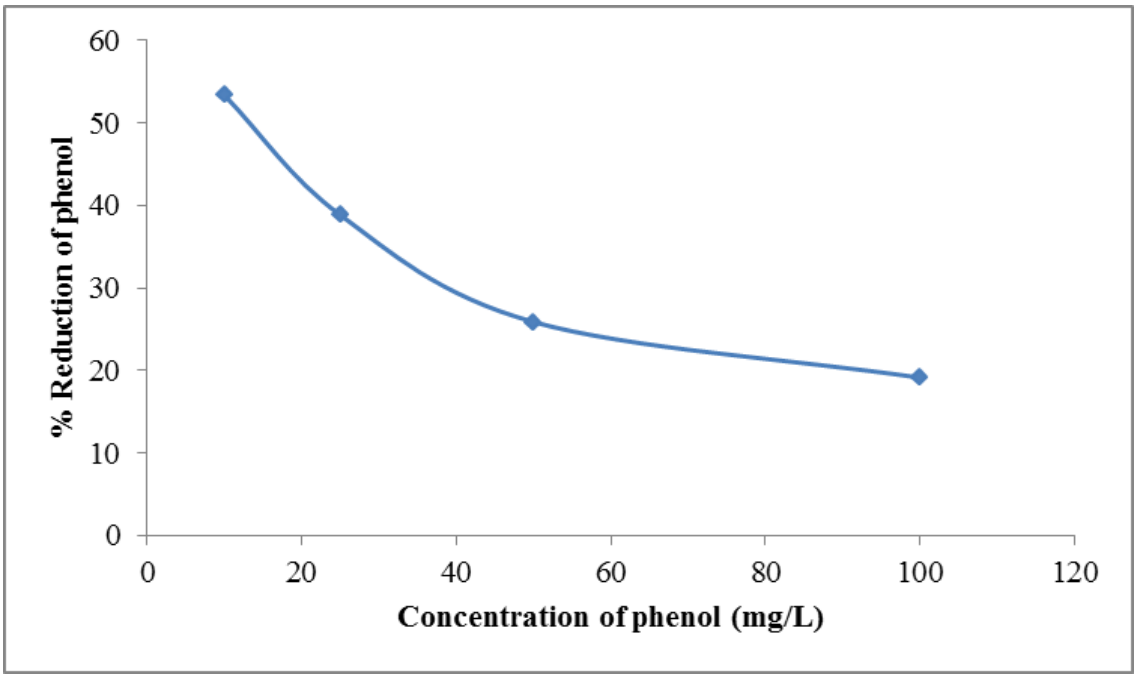

Figure 3.26 Percent reduction of phenol at 2 h in various initial phenol concentrations. Condition: modified TiO_2 grafted chitosan beads at 1% (w/v) of modified TiO_2 = 0.3 g, initial phenol concentration = 10 mg/L, 200 mL, the surface of the solution = 10 cm, stirred reaction mixture, reaction temperature = 30 °C and light intensity = 20 W.

Table 3.2 First order rate constants for phenol photocatalytic degradation at different initial phenol concentrations

Initial phenol concentration (mg/L)	k ($x10^{-3}$ min^{-1})	r
10	6.5	0.998
25	4.3	0.997
50	2.6	0.998
100	1.7	0.997

3.8 Reusability

The modified TiO_2 grafted chitosan beads at 1% (w/v) of modified TiO_2 were washed 3 times with DI water by mechanical shaker for 10 min each time and once with EtOH for 10 min. The washed beads were then dried in oven at 100 °C before being reused in the next cycle under the same condition: 200 mL of 10 mg/L of phenol solution, 10 cm of the distance between light source and the surface of solution, 300 rpm of agitation rate, 10 W of light intensity and irradiation time of 8 h.

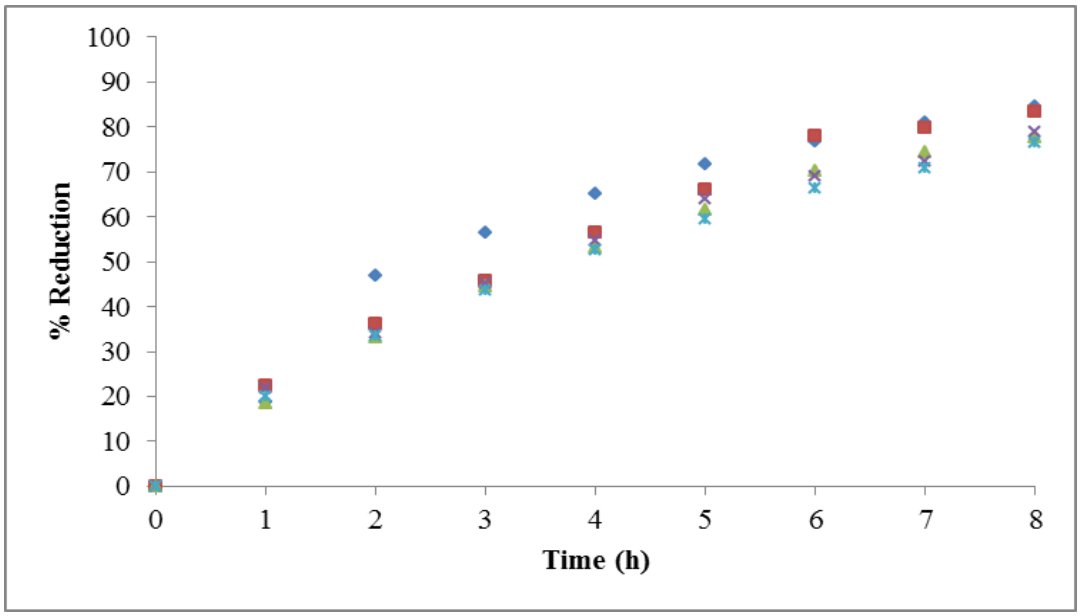

Figure 3.27 The recycling of modified TiO_2 grafted chitosan beads at 1% (w/v) of modified TiO_2: cycle 1(◆), cycle 2 (■), cycle 3(▲), cycle 4 (×) and cycle 5 (✳).

It can be seen in Figure 3.27 that the efficiency of modified TiO_2 grafted chitosan beads to degrade phenol was about 10% decrease when they were reused after 5 times. In each recycling process, the erosion of modified TiO_2 was not observed. The modified TiO_2 grafted chitosan photocatalyst can be used in many cycles due to the properties of TiO_2 that are chemical stability, low solubility and powerful oxidation strength (Hu and Yuan, 2005). It demonstrated that modified TiO_2 grafted chitosan beads is a good material for the removal of phenol.

CHAPTER IV

CONCLUSION

4.1 Conclusion

Chitosan-TiO_2 beads, TiO_2 beads and modified TiO_2 grafted chitosan beads were prepared for the photocatalytic degradation of phenol. SEM picture of chitosan-TiO_2 beads presented a spherical shape in the size range of 500-700 µm. The surface of beads was rather smooth. TiO_2 particles were found to be immobilized in the internal of chitosan beads where Ti element on the surface of chotisan-TiO_2 beads could not be detected by EDX analysis. Chitosan-TiO_2 beads at 1% wt of chitosan showed the best material for phenol removal when compared with other TiO_2 concentrations (0.1, 3, 5, 10% wt of chitosan). It was then used to compare with chitosan-TiO_2 beads in the diameter range 20-100 µm under the same concentration. The result indicated that chitosan-TiO_2 beads in the diameter range of 20-100 µm had less efficiency to remove phenol than chitosan-TiO_2 beads in the size range of 500-700 µm.

To eliminate the negative effect of chitosan from the shielding effect on TiO_2 to react with UV light, TiO_2 spheres were synthesized. Chitosan was acted as a binder to generate spheres before it was removed by calcination at 600 °C. TiO_2 spheres had the same diameter as found in that of chitosan-TiO_2 beads but its surface consisted of TiO_2 particle from 30-300 nm in diameter. XRD pattern of ground TiO_2 spheres exhibited an active anatase form which was effective in photocatalytic degradation

process. The photodegadation of 10 mg/L of phenol 500 mL using commercial TiO_2 powder, chitosan-TiO_2 beads at 1% wt of chitosan and TiO_2 spheres which contain 100 mg of TiO_2 was investigated. TiO_2 spheres showed the least phenol degradation (31%) while commercial TiO_2 powder and chitosan-TiO_2 beads at 1% wt of chitosan represented 75 and 43%, respectively. Moreover, it was fragile and broke easily which might not be proper for recovering process.

Modified TiO_2 grafted chitosan beads were thus, prepared to enhance the phenol degradation efficiency and material reusability. 3-Aminopropyl trietoxysilane and glutaraldehyde were main reagents to modify TiO_2. The optimum condition for the modification of TiO_2 chain was to use 37% (w/v) of glutaraldehyde and the incubation time was 1 h. Various parameters that had an effect on the phenol reduction using modified TiO_2 grafted chitosan beads as a photocatalyst were investigated. The modified TiO_2 at 1% (w/v) showed the best concentration to graft on chitosan beads. The increase of distance between UV lamp and the surface of phenol solution, temperature and light intensity related with the decrease of phenol photodegradation. In addition, the degradation of phenol increased when the initial phenol concentration was decreased. The stirring of solution during the photodegradation process showed that phenol degradation can be improved by approximately 20%. Moreover, the efficiency of modified TiO_2 grafted chitosan beads for phenol degradation still retained at 90% after being reused for 5 cycles.

4.2 Suggestion

Modified TiO_2 grafted chitosan beads can be used as an alternative material for wastewater treatment. In addition, they can be applied to be used in fluidized bed reactor for the removal the pollutants in aqueous or gas phase. The photodegradation of phenol from authentic industrial wastewater using modified TiO_2 grafted chitosan beads should be further determined in order to study the efficiency of the material in wastewater treatment. Furthermore, modified TiO_2 grafted chitosan film can be explored in order to improve its utilization. Other parameters such as pH of reaction, the agitation rate, the position of UV lamp (vertical or horizontal), %DD of chitosan and kinetic study should be further investigated.

REFERENCES

Aksu, Z., and Gönen, F. (2004). Biosorption of phenol by immobilized activated sludge in a continuous packed bed: prediction of breakthrough curves. Process Biochemistry 39: 599-613.

Al-Mahin, A., Chowdhury, M.A.Z., and Fakhruddin, A.N.M. (2010). RW01 Phenol biodegradation by Pseudomonas putida CP1 and A(a). in International Conference on Environmental Aspects of Bangladesh (ICEAB10). Japan.

Andrzejewska, A., Krysztafkiewicz, A., and Jesionowski, T. (2004). Adsorption of organic dyes on the aminosilane modified TiO_2 surface. Dyes and Pigments 62: 121-130.

Aranaz, I., Harris, R., and Heras, A. (2010). Chitosan Amphiphilic Derivatives. Chemistry and Applications. Current Organic Chemistry 14: 308-330.

Bhatkhande, D.S., Pangarkar, V.G., and Beenackers, A.M. (2001). Photocatalytic degradation for environmental applications – a review. Journal of Chemical Technology & Biotechnology 77: 102-116.

Bódalo, A., Gómez, E., Hidalgo, A.M., Gómez, M., Murcia, M.D., and López, I. (2009). Nanofiltration membranes to reduce phenol concentration in wastewater. Desalination 245: 680-686.

Bódalo, A., Gómez, J.L., Gómez, M., León, G., Hidalgo, A.M., and Ruíz, M.A. (2008). Phenol removal from water by hybrid processes: study of the membrane process step. Desalination 223: 323-329.

Brugnerotto, J., Lizardi, J., Goycoolea, F.M., Argüelles-Monal, W., Desbrières, J., and Rinaudo, M. (2001). An infrared investigation in relation with chitin and chitosan characterization. Polymer 42: 3569-3580.

Busca, G., Berardinelli, S., Resini, C., and Arrighi, L. (2008). Technologies for the removal of phenol from fluid streams: A short review of recent developments. Journal of Hazardous Materials 160: 265-288.

Caimei, F., Yanping, S., Yanqin, M., Xiaogang, H., Xinjun, L., and Fangbai, L. (2003). Photocatalytic degradation of phenol in aqueous solution using TiO_2/Ti thin film potocatalytic. Transaction of Nonferrous Metals Society of China 13: 1008-1012.

Carey, F.A. (2000). Organic Chemistry, 4 ed. The McGraw-Hill Companies, Inc., United State of America.

Carp, O., Huisman, C.L., and Reller, A. (2004). Photoinduced reactivity of titanium dioxide. Progress in Solid State Chemistry 32: 33-177.

Castellote, M., and Bengtsson, N. (2011). Principles of TiO_2 Photocatalysis: Application of Titanium Dioxide Photocatalysis to Construction Materials. Springer.

CERAM Research Ltd. (2002). Titanium Dioxide - Titania (TiO_2) [Online]. Available from: http://www.azom.com/article.aspx?ArticleID=1179 [2012, November 28]

Chao, A.C., Shyu, S.S., Lin, Y.C., and Mi, F.L. (2004). Enzymatic grafting of carboxyl groups on to chitosan–to confer on chitosan the property of a cationic dye adsorbent. Bioresource Technology 91: 157-162.

CMR. (2005). Phenol: chemical profile. Chemical Market Reporter: 34-35.

DaNa. (2011). Titanium dioxide [Online]. Available from:http://nanopartikel.info/cms/lang/en/Wissensbasis/Titandioxid [2012, November 26]

Daneshvar, N., Salari, D., Niaei, A., Rasoulifard, M.H., and Khataee, A.R. (2005). Immobilization of TiO_2 nanopowder on glass beads for the photocatalytic decolorization of an azo dye C.I. Direct Red 23. Journal of Environmental Science and Health 40: 1605–1617.

Dawson, A., and Kamat, P.V. (2001). Semiconductor−Metal Nanocomposites. Photoinduced Fusion and Photocatalysis of Gold-Capped TiO_2 (TiO_2/Gold) Nanoparticles. The Journal of Physical Chemistry B 105: 960-966.

De Fávere, V.T., and Hinze, W.L. (2009). Evaluation of the potential of chitosan hydrogels to extract polar organic species from nonpolar organic solvents: Application to the extraction of aminopyridines from hexane. Journal of Colloid and Interface Science 330, 38-44.

Denkbaş, E.B., and Odabaşi, M. (2000). Chitosan microspheres and sponges: Preparation and characterization. Journal of Applied Polymer Science 76, 1637-1643.

Duff, J. (2006). Incinerators and their Health Effects [Online]. Available from: http://ideaireland.org/library/incinerators-and-their-health-effects [2013, February 7]

Dutta, P.K., Dutta, J., and Tripathi, V.S. (2004). Chitin and chitosan: Chemistry, properties and applications. Journal of Scientific and Industrial Research 63: 20-31.

Egorov, V.M., Smirnova, S.V., and Pletnev, I.V. (2008). Highly efficient extraction of phenols and aromatic amines into novel ionic liquids incorporating quaternary ammonium cation. Separation and Purification Technology 63: 710-715.

Einaga, H., Futamura, S., and Ibusuki, T. (1999). Photocatalytic decomposition of benzene over TiO_2 in a humidified airstream. Physical Chemistry Chemical Physics 1: 4903-4908.

Emeline A.V., S.A., Ryabchuk V.K., and Serpone N. (2001). Photo-induced processes in heterogeneous nanosystems from photoexcitation to interfacial chemical transformations. International Journal Photoenergy 3: 1-16.

Folsom, B.R., Chapman, P.J., and Pritchard, P.H. (1990). Phenol and trichloroethylene degradation by Pseudomonas cepacia G4: kinetics and interactions between substrates. Applied and Environmental Microbiology 56: 1279–1285.

Gao, Y., Masuda, Y., Peng, Z., Yonezawa, T., and Koumoto, K. (2003). Room temperature deposition of a TiO_2 thin film from aqueous peroxotitanate solution. Journal of Materials Chemistry 13: 608-613.

Greenpeace Southeast Asia. (2010). Wastewater in Thailand [Online]. Available from: http://www.thaipost.net/sunday/210210/18247 [2010, February 21]

Hashimoto, K., Irie, H., and Fujishima, A. (2005). TiO_2 Photocatalysis: A Historical Overview and Future Prospects. Japanese Journal of Applied Physics 44: 8269-8285.

Horikoshi, S.W.N., Mukae M., Hidaka, H. and Serpone, N. (2001). Mechanistic examination of titania-photocatalyzed oxidation of ethanolamines. New Journal of Chemistry 25, 999-1005.

HSDB. (2008). Phenol hazardous substances data bank [Online]. Available from: http://toxnet.nlm.nih.gov./cgi-bin/sis/search/f?./temp/~01RkhY:1 [2013, January 4]

Hu, Y., and Yuan, C. (2005). Low-temperature preparation of photocatalytic thin films from anatase sols. Journal of Crystal Growth 274, 563-568.

IRIS. (2002). Phenol. [Online]. Available from: http://www.epa.gov/iris/subst/index.html [2013, January 4]

Juang, R. S., Huang, W. C., and Hsu, Y. H. (2009). Treatment of phenol in synthetic saline wastewater by solvent extraction and two-phase membrane biodegradation. Journal of Hazardous Materials 164: 46-52.

Keith, L.H., and Telliard, W.A. (1979). Priority pollutants I - a perspective view. Environmental Science and Technology 13: 416-423.

Khachatryan, K., Smirnova, S., Torocheshnikova, I., Shvedene, N., Formanovsky, A., and Pletnev, I. (2005). Solvent extraction and extraction–voltammetric determination of phenols using room temperature ionic liquid. Analytical Bioanalytical Chemistry 381: 464-470.

Kim, T.W., and Lee, M.J. (2010). Effect of pH and Temperature for Photocatalytic Degradation of Organic Compound on Carbon-coated TiO_2. Journal of Advanced Engineering and Technology 3: 193-198.

Konstantinou, I.K., and Albanis, T.A. (2004). TiO_2-assisted photocatalytic degradation of azo dyes in aqueous solution: kinetic and mechanistic investigations: A review. Applied Catalysis B: Environmental 49: 1-14.

Lam, S.M., Sin, J.C., and Mohamed, A. (2010). Parameter effect on photocatalytic degradation of phenol using TiO_2-P25/activated carbon (AC). Korean Journal of Chemical Engineering 27: 1109-1116.

Laoufi, N.A., Tassalit, D., and Bentahar, F. (2008). The degradation of phenol in water solution by TiO_2 photocatalysis in a helical reactor. Global NEST Journal 10: 404-418.

Larnoy, E., Eikenes, M., and Militz, H. (2011). Detection of chlorine-labelled chitosan in Scots pine by energy-dispersive X-ray spectroscopy. Wood Science and Technology 45: 103-110.

Lee, M.S., Huang, C., Lee, K.R., Pan, J.R., and Chang, W.K. (2008). Factors affecting phenol transfer through polydimethylsiloxane composite membrane. Desalination 234: 416-425.

Lee, J.M., Kim, M.S., and Kim, B.W. (2004). Photodegradation of bisphenol-A with TiO_2 immobilized on the glass tubes including the UV light lamps. Water Research 38: 3605-3613.

Li, J., Chen, C., Zhao, J., Zhu, H., and Ding, Z. (2002). Photodegradation of dye pollutants on TiO_2 pillared bentonites under UV light irradiation. Science in China Series B: Chemistry 45, 445-448.

Liao, C.H., Huang, C.W., and Wu, J.C.S. (2012). Hydrogen Production from Semiconductor-based Photocatalysis via Water Splitting. Catalysts 2, 490-516.

Ling, C.M., Mohamed, A.R., and Bhatia, S. (2004). Performance of photocatalytic reactors using immobilized TiO_2 film for the degradation of phenol and methylene blue dye present in water stream. Chemosphere 57: 547-554.

Liu, L.F., Zhang, P.H., and Yang, F.L. (2010). Adsorptive removal of 2,4-DCP from water by fresh or regenerated chitosan/ACF/TiO_2 membrane. Separation and Purification Technology 70: 354-361.

Lupetti, K.O., Rocha, F.R.P., and Fatibello-Filho, O. (2004). An improved flow system for phenols determination exploiting multicommutation and long pathlength spectrophotometry. Talanta 62: 463-467.

Mahvi, A.H., Maleki, A., Alimohamadi, M., and Ghasri, A. (2007). Photo-oxidation of phenol in aqueous solution: Toxicity of intermediates. Korean Journal of Chemical Engineering 24: 79-82.

Mi, F.L., Shyu, S.S., Wong, T.B., Jang, S.F., Lee, S.T., and Lu, K.T. (1999). Chitosan–polyelectrolyte complexation for the preparation of gel beads and controlled release of anticancer drug. II. Effect of pH-dependent ionic crosslinking or interpolymer complex using tripolyphosphate or polyphosphate as reagent. Journal of Applied Polymer Science 74: 1093-1107.

Michałowicz, J., and Duda, W. (2007). Phenols–Sources and Toxicity. Polish Journal of Environmental Studies 16: 347-362.

Minsker, K.S., Zakharov, V.P., and Berlin, A.A. (2001). Plug-Flow Tubular Turbulent Reactors: A New Type of Industrial Apparatus. Theoretical Foundations of Chemical Engineering 35: 162-167.

Nawi, M.A., Jawad, A.H., Sabar, S., and Ngah, W.S.W. (2011). Immobilized bilayer TiO_2/chitosan system for the removal of phenol under irradiation by a 45 watt compact fluorescent lamp. Desalination 280: 288-296.

Nawi, M.A., Sabar, S., Jawad, A.H., Sheilatina, and Ngah, W.S.W. (2010). Adsorption of Reactive Red 4 by immobilized chitosan on glass plates: Towards the design of immobilized TiO_2–chitosan synergistic photocatalyst-adsorption bilayer system. Biochemical Engineering Journal 49: 317-325.

No, H.K., and Meyers, S.P. (2000). Application of Chitosan for Treatment of Wastewaters. Reviews of Environmental Contamination and Toxicology (Ware, G., Ed.), pp 1-27. Springer, New York.

Nur, H. (2006). Modification of titanium surface species of titania by attachment of silica nanoparticles. Materials Science and Engineering: B 133: 49-54.

Patra, S., and Munichandraiah, N. (2008). Electro-oxidation of phenol on polyethylenedioxythiophene conductive-polymer-deposited stainless steel substrate. Journal of the Electrochemical Society 155(3): F23-F30.

Pillai, S., Seery, M., Nolan, N., Pelaez, M., and Kontosd, A.G. (2012). A Review on the Visible Light Active Titanium Dioxide Photocatalysts for Environmental Applications. Applied Catalysis B 125: 331– 349.

Pollution Control Department. (2010). The standard level of industrial wastewater [Online]. Available from: http://www.pcd.go.th/info_serv/reg_std_water04.html [2013, March 7]

Puzenat, E., and Pichat, P. (2003). Studying TiO_2 coatings on silica-covered glass by O_2 photosorption measurements and FTIR–ATR spectrometry: Correlation with the self-cleaning efficacy. Journal of Photochemistry and Photobiology A: Chemistry 160: 127-133.

Qourzal, S.T.M., Assabbane A., Bouamrane A., Nounah A., Laanab L., and Ait-Ichou Y. (2006). Preparation of TiO_2 Photocatalyst Using $TiCl_4$ as a Precursor and its Photocatalytic Performance. Journal of Applied Sciences 6*:* 1553-1559.

Quan, X., Zhao, X., Chen, S., Zhao, H., Chen, J., and Zhao, Y. (2005). Enhancement of p,p′-DDT photodegradation on soil surfaces using TiO_2 induced by UV-light. Chemosphere 60, 266-273.

Ravi Kumar, M.N.V. (2000). A review of chitin and chitosan applications. Reactive and Functional Polymers 46: 1-27.

Rinaudo, M. (2006). Chitin and chitosan: Properties and applications. Progress in Polymer Science 31: 603-632.

Robertson, P.K.J. (1996). Semiconductor photocatalysis: an environmentally acceptable alternative production technique and effluent treatment process. Journal of Cleaner Production 4: 203-212.

Rubin, E., Rodriguez, P. (2006). Biosorption of phenolic compounds by the brown alga sargassum muticum. Journal of Chemical Technology Biotechnology 81: 1093-1099.

San, N., Hatipoglu, A., Kocturk, G., and Cinar, Z. (2001). Prediction of primary intermediates and the photodegradation kinetics of 3-aminophenol in aqueous TiO_2 suspensions. Journal of Photochemistry and Photobiology A: Chemistry 139, 225-232.

Schellin, M., and Popp, P. (2005). Membrane-assisted solvent extraction of seven phenols combined with large volume injection–gas chromatography–mass spectrometric detection. Journal of Chromatography A 1072: 37-43.

Shahidi, F., Arachchi, J.K.V., and Jeon, Y.J. (1999). Food applications of chitin and chitosans. Trends in Food Science & Technology 10: 37-51.

Shao, J., Ge, H., and Yang, Y. (2007). Immobilization of polyphenol oxidase on chitosan–SiO_2 gel for removal of aqueous phenol. Biotechnology Letters 29: 901-905.

Shawabkeh, R.A., Khashman, O.A., and Bisharat, G.I. (2010). Photocatalytic degradation of phenol using Fe-TiO_2 by different illumination sources. International Journal of Chemistry 2: 10-12.

Simi, C.K., and Abraham, T.E. (2009). Nanocomposite based on modified TiO_2–BSA for functional applications. Colloids and Surfaces B: Biointerfaces 71: 319-324.

Siqueira, R.L., Yoshida, I.V.P., Pardini, L.C., and Schiavon, M.A. (2006). Poly(borosiloxanes) as precursors for carbon fiber ceramic matrix composites. Materials Research 10: 186-193.

Sobczyński, A., Duczmal, Ł., and Zmudziński, W. (2004). Phenol destruction by photocatalysis on TiO_2: an attempt to solve the reaction mechanism. Journal of Molecular Catalysis A: Chemical 213: 225-230.

Subramanian, M., and Kannan, A. (2008). Effect of dissolved oxygen concentration and light intensity on photocatalytic degradation of phenol. Korean Journal of Chemical Engineering 25: 1300-1308.

Tancredi, N., Medero, N., Möller, F., Píriz, J., Plada, C., and Cordero, T. (2004). Phenol adsorption onto powdered and granular activated carbon, prepared from Eucalyptus wood. Journal of Colloid and Interface Science 279: 357-363.

Thamaphat, K., Limsuwan, P., and Ngotawornchai, B. (2008). Phase Characterization of TiO_2 Powder by XRD and TEM. Kasetsart Journal: Natural Science 42, 357-361.

Thiruvenkatachari, R., Vigneswaran, S., and Moon, I.S. (2008). A review on UV/TiO_2 photocatalytic oxidation process (Journal Review). Korean Journal of Chemical Engineering 25: 64-72.

Tong, T., Zhang, J., Tian, B., Chen, F., and He, D. (2008). Preparation and characterization of anatase TiO_2 microspheres with porous frameworks via controlled hydrolysis of titanium alkoxide followed by hydrothermal treatment. Materials Letters 62: 2970-2972.

Trillas, M., Peral, J., and Domènech, X. (1999). Photocatalyzed Degradation of Phenol, 2,4-Dichlorophenol, Phenoxyacetic Acid and 2,4-Dichlorophenoxyacetic Acid over Supported TiO_2 in a Flow System. Journal of Chemical Technology & Biotechnology 67: 237-242.

Tseng, C. (2009). Uses of chitosan [Online]. Available from: http://www.france-chitine.com/util.e.html [2012, October 29]

Vega, A.A., Keshmiri, M., and Mohseni, M. (2011). Composite template-free TiO_2 photocatalyst: Synthesis, characteristics and photocatalytic activity. Applied Catalysis B: Environmental 104: 127-135.

Vinu, R., and Madras, Gr. (2010). Environmental remediation by photocatalysis. Journal of the Indian Institute of Science 90: 189-230.

Wagner, M., and Nicell, J.A. (2002). Detoxification of phenolic solutions with horseradish peroxidase and hydrogen peroxide. Water Research 36: 4041-4052.

Wang, H., Fang, Y., Ding, L., Gao, L., and Hu, D. (2003). Preparation and nitromethane sensing properties of chitosan thin films containing pyrene and beta-cyclodextrin units. Thin Solid Films 440: 255-260.

Wang, R., Hashimoto, K., and Fujishima, A. (1997). Light-induced amphiphilic surfaces. Nature 388: 431-432.

Weis, H., Fernandez, A., and Kisch, H. (2001). Electronic Semiconductor–Support Interaction-A Novel Effect in Semiconductor Photocatalysis. Angewandte Chemie International Edition 40: 3825-3827.

WHO. (1994). Phenol. Environmental health criteria 161. Geneva, Switzerland: United Nations Environment Programme. International Labour Organisation. World Health Organization.

Wong, C.L., Tan, Y.N., and Mohamed, A.R. (2011). Photocatalytic Degradation of Phenol Using Immobilized TiO_2 Nanotube Photocatalysts. Journal of Nanotechnology 2011: 1-9.

Wongkaew, A., Jansome, W., Sawaengmit, S.K.N., and Mitpapan, S. (2010). Synthesis of Nanoparticles of Mixed Oxides Containing Titanium Cerium Silver and Silicon: Phase Transformation. Energy Research Journal 1, 73-77.

Wu, C., Liu, X., Wei, D., Fan, J., and Wang, L. (2001). Photosonochemical degradation of Phenol in water. Water Research 35: 3927-3933.

Wu, F.C., Tseng, R.L., and Juang, R.S. (2000). Comparative adsorption of metal and dye on flake-and bead-types of chitosans prepared from fishery wastes. Journal of Hazardous Materials 73: 63-75.

Wu, H.S., and Li, C.C. (2008). Kinetic study of phenol recovery using phase-transfer catalysis in horizontal membrane reactor. Chemical Engineering Journal 144(3): 502-508.

Yu, Q.L., and Brouwers, H.J.H. (2009). Indoor air purification using heterogeneous photocatalytic oxidation. Part I: Experimental study. Applied Catalysis B: Environmental 92: 454-461.

Zainal, Z., Hui, L.K., Hussein, M.Z., Abdullah, A.H., and Hamadneh, I.R. (2009). Characterization of TiO_2–Chitosan/Glass photocatalyst for the removal of a monoazo dye via photodegradation–adsorption process. Journal of Hazardous Materials 164: 138-145.

Zhang, D., Qi, L., Ma, J., and Cheng, H. (2002). Formation of crystalline nanosized titania in reverse micelles at room temperature. Journal of Materials Chemistry 12: 3677-3680.

Zheng, S.Y.Z., Jo D.H., and Park Y.H. (2004). Removal of chlorophenols from groundwater by chitosan sorption. Water Research 38: 2314-2321.

APPENDICES

Appendix A

Calculation of %reduction of phenol

A1 Calibration curve of phenol

The concentration versus absorbance of phenol solution at 510 nm was presented in Table A1. They show a linear relationship with the correlation coefficient = 0.9996 (Figure A1).

Table A1 Absorbance of phenol solution determined by UV-Vis spectrophotometer

Concentration (mg/L)	Absorbance (510 nm)
0	0
2.5	0.11
5	0.24
7.5	0.35
10	0.48
20	0.96
25	1.22

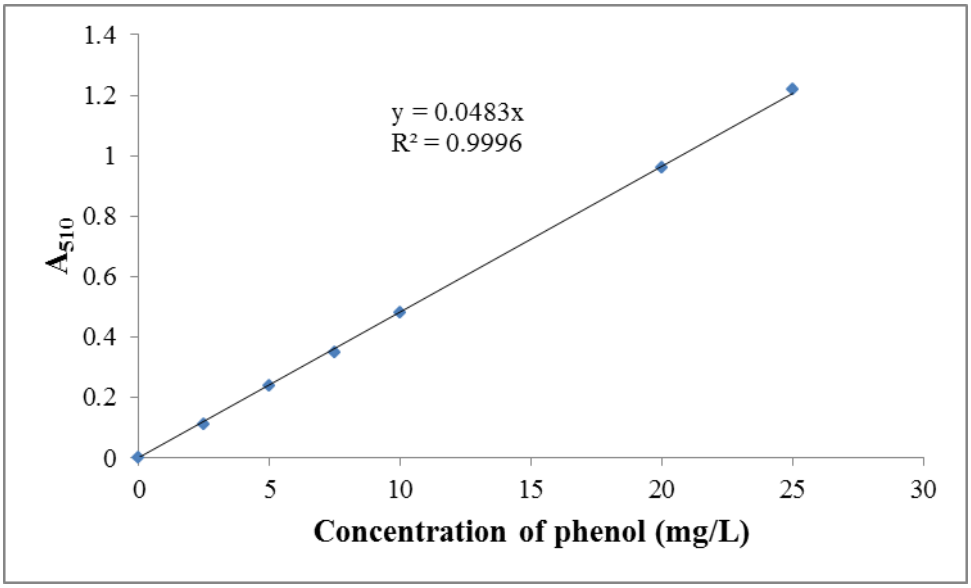

Figure A1 Standard calibration curve of phenol.

A2 Example of the calculation of phenol reduction

Effect of TiO_2 dosage of chitosan-TiO_2 beads on phenol photodegradation

Experimental condition	
Amount of 10 mg/L of phenol	500 mL
Amount of chitosan-TiO_2 at 1 % wt of chitosan	0.5 g
Distance between light source and surface of solution	15 cm

The calibration curve of phenol at the concentration of 10 to 25 mg/L showed the straight line with the equation:

$$Y = 0.0483X$$

Where y = Absorbance of phenol

X = Concentration of phenol

Table A2 Effect of chitosan-TiO_2 beads at TiO_2 1 % wt of chitosan on phenol photodegradation

Time (h)	A510	Concentration (mg/L)	%Reduction
0	0.4826	9.99	0
1	0.4386	9.08	9.11
2	0.4218	8.73	12.61
3	0.3907	8.09	19.02
4	0.3692	7.64	23.52
5	0.3559	7.37	26.23
6	0.3357	6.95	30.43
7	0.3220	6.67	33.23
8	0.3107	6.43	35.64

1.1 Initial concentration of phenol

From equation Y = 0.0483X

Initial phenol concentration = Absorbance / 0.0483

= 0.4826/0.0483

= 9.99 mg/L

1.2 Concentration of phenol after 8 h

From equation Y = 0.0483X

Concentration of phenol = 0.3107/0.0483

= 6.43 mg/L

1.3 %Reduction of phenol

% Reduction = $[(C_0-C_t)/C_0]*100$

Where C_0 = Initial phenol concentration

C_t = Concentration of phenol in solution at a given time.

%Reduction of phenol at 8 h = [(9.99-6.43)/9.99)*100

= 35.64

Appendix B

Calculation of rate constant

B1 Example of the calculation of rate constant

First-order kinetic model; $\ln C_t = -kt\ \mathrm{C} + \ln C_0$

where C_0 = The initial concentration and (mg/L)

C_t = The concentration of phenol at time t (mg/L)

k = Rate constant (min^{-1})

Plot $-\ln(C_t/C_0)$ versus reaction time (t) yields a straight line, the slope is rate constant (k) as showed in Figure B. The rate constant was equal to 9.5×10^{-3} min^{-1}.

Table B1 Effect of light intensity

UV light intensity (W)	**Time (h)**	**Concentration (mg/L)**	C_t/C_0	$-\ln(C_t/C_0)$
40	0	9.93	1	0
	0.5	7.84	0.79	0.24
	1	6.37	0.64	0.45
	1.5	5.13	0.52	0.65
	2	3.70	0.37	0.99
	3	2.12	0.21	1.56
	4	1.09	0.11	2.21
	5	0.57	0.057	2.86

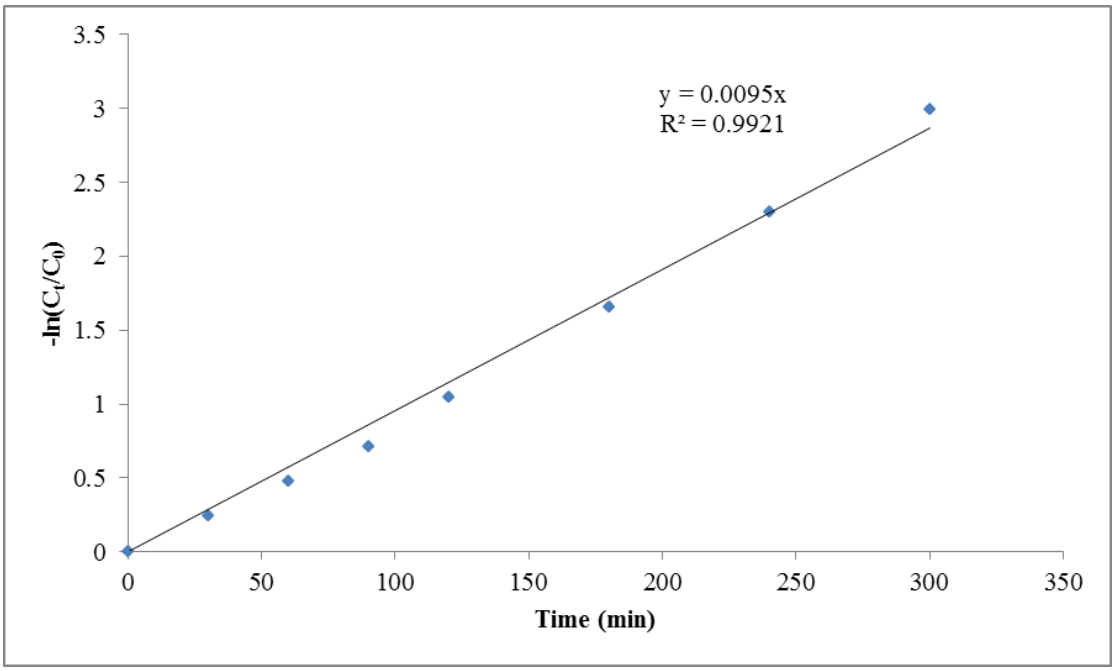

Figure B1 Plot of ln C_t/C_0 vs. time for photodegradation of phenol at 40 W.

VITAE

Miss Punnida Nonsuwan was born on September 27th, 1987 in Kalasin, Thailand. She received a Bachelor Degree of Science, major in Chemistry from Silpakorn University in 2009. Since 2010 she has been a graduate student in the program of Biotechnology, Faculty of Science, Chulalongkorn University.